

# Analytical Insights into Constant-Roll Condition: Extending the Paradigm to Non-Canonical Models

S. Mohammad Ahmadi,<sup>a</sup> Nahid Ahmadi,<sup>a</sup> and Mehdi Shokri<sup>a,b,c</sup>

<sup>a</sup>Department of Physics, University of Tehran, Karegar Ave North, Tehran 14395-547, Iran

<sup>b</sup>School of Physics, Damghan University, P. O. Box 3671641167, Damghan, Iran

<sup>c</sup>Canadian Quantum Research Center, 204-3002 32 Ave Vernon, BC V1T 2L7 Canada

E-mail: [mohammadahmadi@ut.ac.ir](mailto:mohammadahmadi@ut.ac.ir), [nahmadi@ut.ac.ir](mailto:nahmadi@ut.ac.ir),  
[mehdishokriphysics@gmail.com](mailto:mehdishokriphysics@gmail.com)

**Abstract.** In this work, we explore the prospect of generalizing the constant-roll condition in canonical inflationary model to non-canonical models. To find a natural generalization, we focus on three manifestations of this condition and construct constant-roll models corresponding to each manifestation. These models are not equivalent but reduce to the familiar constant-roll model in canonical limit. To showcase the applicability of our generalized mechanism, we examine a specific class of non-canonical models, which can be viewed as extensions of  $k/G$  inflation. We conduct a comprehensive analytical examination of the model, elucidating instances where our constant-roll conditions yield disparate outcomes and when they exhibit analogies. We also apply our findings to scrutinize another kinetically driven inflationary model within the constant-roll framework. We demonstrate that each of our constant-roll conditions leads to a unique set of solutions. Afterward, we construct a four-stage constant-roll kinetically driven inflation (or "constant  $k$  inflation" for short) capable of producing primordial black holes, satisfying CMB constraints, and providing a graceful exit from inflation. Employing numerical methods, we analyze this scenario to elucidate how altering the constant-roll condition impacts the power spectrum and the model's dynamics.

---

## Contents

<b>1</b>	<b>Introduction</b>	<b>1</b>
<b>2</b>	<b>Canonical Constant-Roll Inflation</b>	<b>3</b>
<b>3</b>	<b>Constant-Roll Condition in Non-Canonical Models</b>	<b>11</b>
<b>4</b>	<b>Constant-Roll and Propagation Inflation</b>	<b>13</b>
4.1	Field-Constant-Roll Condition	14
4.2	Hubble-Constant-Roll and Potential-Constant-Roll Conditions	16
4.3	An Example: k/G Inflation	17
<b>5</b>	<b>Constant-Roll Kinetically Driven Inflation</b>	<b>25</b>
5.1	Quasi-Canonical Phase	26
5.2	Exact Solutions	28
5.3	PBH Formation	29
<b>6</b>	<b>Summary and Conclusion</b>	<b>32</b>
<b>A</b>	<b>The Turning Point of <math>n_s</math> and <math>f_{NL}^{re}</math></b>	<b>33</b>

---

## 1 Introduction

It is widely accepted that inflation provides the best explanation for the early universe [1–7]. It proposes that a small epoch of accelerated expansion at very early universe can potentially smooth out inhomogeneities and anisotropies and reduce the curvature of space. In addition to explaining some of our fundamental questions, such as the flatness, horizon, and monopole problems, it suggests a mechanism for the generation of quantum perturbations in the early universe. There have been countless studies conducted on inflation, and observations of the cosmic microwave background (CMB) and of the large scale structure (LSS) of our universe have confirmed the predictions of inflation. In conventional inflationary models, a scalar field  $\phi$  whose potential energy dominates the energy density of the universe is responsible for an accelerated expansion. The spectral index of canonical single field inflationary model is shown to be consistent with observational data in the slow-roll and ultra slow-roll (USR) regimes [8–10]. Nevertheless, the detailed dynamical characteristics of inflation is still obscure. Motivated by this, a one-parameter class of models (defined by the relation  $\ddot{\phi} = \beta H \dot{\phi}$  or equivalently  $\ddot{H} = 2\beta H \dot{H}$ , where  $\beta$  is the free parameter of the model) was proposed in [11] to unify simple scenarios like slow-roll and USR, and construct or maybe rule out many models of inflation. Later on the same class of models was studied in more detail and referred to as constant-roll inflation [12]. In the canonical constant-roll scenario, slow-roll behavior can be observed when  $\beta \rightarrow 0$  and a constant USR potential at  $\beta = -3$ . Therefore, it can be considered a generalization of USR inflation.

The constant-roll scenario has attracted a great deal of attention in recent years. The novelty is that the equations of motion of the canonical constant-roll model can be solved analytically. Many instances of non-canonical constant-roll models can also be treated analytically. Its flexibility is another noteworthy feature of the model; changing the constant-roll

parameter  $\beta$  will allow one to switch between slow-roll and USR regimes. Different aspects of the canonical constant-roll model has been studied in [11–26]. Furthermore, numerous studies have been conducted on non-minimal and non-canonical models under the constant-roll assumption [27–56]. The constant-roll scenario may also be a candidate for the formation of primordial black holes, which has been the subject of considerable number of research [57–66].

Although many studies have attempted to generalize the action of the constant-roll model, some authors focused on the generalization of the constant-roll condition [25–27]. For example, authors in reference [25] add a new free parameter to the constant-roll condition by writing  $\ddot{\phi} = \dot{\phi}(\beta H + \alpha)$ . Using this condition, we can recover the conventional constant-roll condition for  $\alpha = 0$ , while achieving a broader class of constant-roll potentials for  $\alpha \neq 0$ .

The generalization of constant-roll condition is much more intriguing in non-canonical models. In a non-canonical model, unlike the canonical case,  $\beta = -3$  does not always lead to USR. Therefore, to study the USR limit of the model, an special form of generalized constant-roll condition is required. A good example of such a generalization can be found in [27]. The purpose of their study was to investigate the  $f(R)$  gravity under the assumption of a constant rate of roll. For this purpose they defined the constant-roll condition as  $\ddot{F} = \beta H_J \dot{F}$ , where  $F = df/dR$  and subscript  $J$  denotes the Jordan frame. With this condition, USR and slow-roll regimes amount to  $\beta \rightarrow -3$  and  $\beta \rightarrow 0$  limits, respectively, and the model is considered to be a natural generalization of USR. The point is that such a generalization can be produced in many ways. One can choose one or another constant-roll condition based on simplicity or aesthetic elegance. In the study of non-canonical models, it is also possible to define an infinite number of distinct constant-roll conditions, all leading to the conventional constant-roll condition  $\ddot{\phi} = \beta H \dot{\phi}$  in the canonical limit, yet exhibit varied implications upon departure from the canonical framework. As a result of this freedom, constant-roll condition can be defined in accordance with the needs of the individual to study the desired physical concepts.

In this work, we use different manifestations of constant-roll inflation in order to impose three types of constant-roll conditions on a general  $P(X)$  model. Our first approach is based on the fact that the constant-roll condition is defined to ensure a constant rate of field roll. The second approach establishes constant-roll condition that leads to a constant  $\epsilon_2$ , and for our third constant-roll condition, we introduce the condition that corresponds to the USR as  $\beta$  approaches  $-3$ . Next, we present and carefully examine a novel class of constant-roll and propagation inflation (which naturally extends the concept of k/G inflation [67], as it results in k/G inflation when sound speed is one) in order to demonstrate how a model can be affected by changing the constant-roll condition. While each constant-roll condition generally leads to distinct solutions and consequences, we demonstrate that specific limits can be identified where all three conditions converge toward a quasi-canonical phase. We use the term 'quasi-canonical', in the sense that at these limits slow-roll parameters and consequently the perturbations of the model mimics the canonical model while the action generally differs from the canonical case.

We then broaden our horizons by investigating another model with non-standard kinetic term such as  $k$  inflation [68–73] under the constant-roll assumption. We demonstrate that the model can naturally transition between two phases: the standard canonical constant-roll case and a novel phase we call the large  $\gamma$  phase. While the characteristics of the canonical phase remain independent of the specific constant-roll condition employed, the large  $\gamma$  phase and the transition dynamics between the two phases are highly dependent on the chosen constant-roll

condition. To provide a more vivid demonstration of the constant-roll condition’s impact on the model’s dynamics, we introduce a four-stage constant scenario with the potential to give rise to primordial black holes. We discuss how our scenario aligns with CMB constraints and facilitates a graceful exit from inflation. We conclude that altering the constant-roll condition can modify the resulting power spectrum, thereby significantly influencing primordial black holes abundance.

This paper is arranged as follows. In Section 2, we review the canonical constant-roll model. In Section 3, we introduce three distinct constant-roll conditions to implement constant-roll constraints in non-canonical models. We explore the applications of our generalized constant-roll mechanism by examining a class of non-canonical model in section 4. We carefully scrutinize the interrelationships among our three constant-roll conditions, elucidating their analogies and distinctions. Section 5 investigates another non-canonical model as an example of models that show different dynamical behavior under three defined constant-roll conditions. We then construct a multi-stage constant  $k$  scenario capable of producing primordial black holes. Numerical calculations of the power spectrum and other dynamic parameters are presented to understand how different generalizations of the constant-roll condition can impact the model. We conclude in section 6.

## 2 Canonical Constant-Roll Inflation

In this section we present a review of the canonical constant-roll model [11–15]. We determine all possible constant-roll solutions and discuss the primordial perturbations resulting from them. In the next sections, when we discuss more general constant-roll cases, we will follow the same steps as here.

We consider the simplest inflationary scenario that contains a single scalar field with the standard kinetic term minimally coupled to gravity. The dynamics of this model is described by the well-known Friedmann and Klein-Gordon equations<sup>1</sup>,

$$3H^2 = \frac{\dot{\phi}^2}{2} + V(\phi), \quad (2.1)$$

$$\ddot{\phi} + 3H\dot{\phi} + V_{,\phi} = 0, \quad (2.2)$$

where a comma stands for a partial derivative, and a dot stands for cosmic time derivative. Using these equations, one can find a differential equation in terms of the inflaton field and Hubble parameter

$$\dot{H} = -\frac{\dot{\phi}^2}{2}. \quad (2.3)$$

To characterize the evolution of the background, slow-roll parameters are defined as follows:

$$\epsilon_1 \equiv \frac{d \ln H}{dN}, \quad \epsilon_{j+1} \equiv \frac{d \ln \epsilon_j}{dN}, \quad (2.4)$$

where  $j$  is a positive integer, and  $N$  is the number of e-fold defined as  $dN \equiv d \ln a = H dt$ . Using definition (2.4) together with equation (2.3) and its derivative, the second slow-roll parameter can be written as

$$\epsilon_2 = 2\epsilon_1 + \frac{\ddot{H}}{H\dot{H}}. \quad (2.5)$$

---

<sup>1</sup>Throughout the paper we work in Planck units where  $c = G = \hbar = 1$ .

Let us now consider a class of models in which the second term on the right-hand side of equation (2.5) remains constant during the inflationary epoch

$$\beta = \frac{\ddot{H}}{2H\dot{H}} = \frac{\ddot{\phi}}{H\dot{\phi}} = \frac{\dot{V}}{2H\dot{H}} - 3, \quad (2.6)$$

where  $\beta$  is a real constant, and for the last two equity we have used equations (2.2) and (2.3). Equation (2.6) is called the *constant-roll condition* and  $\beta$  is the *constant-roll parameter*. From (2.6) we notice that  $\beta$  constrains not only the rate of change of  $\dot{H}$  and  $\dot{\phi}$ , but also the rate of change of potential compared to that of  $H^2$ . Based on equations (2.5) and (2.6), and assuming that  $\epsilon_1$  is small,  $\epsilon_2$  can be approximated as  $\epsilon_2 \approx 2\beta$ . If we set the parameter  $\beta$  to zero, it is similar to the slow-roll case when we neglect the  $\dot{\phi}$  in the Klein-Gordon equation (2.2). If parameter  $\beta$  is set to  $-3$ , it leads to  $V_{,\phi} = 0$  case which is dubbed as *ultra slow-roll inflation* (USR) [8–10]. In canonical models, the three purportedly distinct expressions for  $\beta$  are actually "the same" related by the system of equations (2.1)–(2.3).

In this work, we often find it more convenient to work with number of e-fold  $N$  rather than cosmic time  $t$ . Writing all time derivatives in equations (2.1), (2.2), (2.3), and (2.6) in terms of  $N$ , we have

$$3H^2 = \frac{H^2\phi_{,N}^2}{2} + V, \quad (2.7)$$

$$H_{,N} = -\frac{H\phi_{,N}^2}{2}, \quad (2.8)$$

$$H^2\phi_{,NN} + HH_{,N}\phi_{,N} + 3H^2\phi_{,N} + V_{,\phi} = 0, \quad (2.9)$$

$$HH_{,NN} + (H_{,N})^2 = 2\beta HH_{,N}. \quad (2.10)$$

By integrating equation (2.10) for the Hubble parameter we find:

$$H^2 = C_1 \left( C_2 e^{2\beta N} + 1 \right), \quad (2.11)$$

where in general  $C_1$  and  $C_2$  are two arbitrary complex numbers. However, since the Hubble parameter is real, only real values for  $C_1$  and  $C_2$  are physically feasible. For simplicity, we rewrite these constants as  $C_1 = \text{sgn}(C_1)|C_1| = \text{sgn}(C_1)M^2$  and  $C_2 = \text{sgn}(C_2)|C_2| = \text{sgn}(C_2)e^{2\beta N_0}$ , where  $N_0$  is a real constant,  $M$  is a positive real constant, and  $\text{sgn}$  is the sign function. From this, we can deduce that the modulus of  $C_2$  acts as a time shift. Therefore, without loss of generality, we can assume that inflation starts at  $N = N_{\text{ini}}$  and set  $N_0 = 0$  (or  $|C_2| = 1$ ). Taking this into account, relation (2.11) can be written as  $H^2 = M^2 \text{sgn}(C_1) (\text{sgn}(C_2) e^{2\beta N} + 1)$ , which leaves us with the following choices:

$$H^2 = -M^2 \left( 1 + e^{2\beta N} \right), \quad (2.12)$$

$$H^2 = M^2 \left( 1 + e^{2\beta N} \right), \quad (2.13)$$

$$H^2 = M^2 \left( 1 - e^{2\beta N} \right), \quad (2.14)$$

$$H^2 = M^2 \left( e^{2\beta N} - 1 \right). \quad (2.15)$$

We first note that the right-hand side of solution (2.12) is always negative, which leads to an imaginary Hubble parameter, and is therefore unacceptable. In contrast, solution (2.13)

always results in a real Hubble parameter. For solutions (2.14) and (2.15), the Hubble parameter is real only when we have  $\beta N < 0$  and  $\beta N > 0$ , respectively. Note that cases (2.14) and (2.15) are zero at  $N = 0$ , which is the singular point of differential equation (2.10). Therefore, our solutions are not viable in the vicinity of this point.

As we will see later, despite the similarities between solutions (2.13), (2.14), and (2.15), they describe a valid inflationary dynamic for different ranges of  $N$  and parameter  $\beta$ . Our goal here is to find all physically possible inflationary solutions whether or not they are dynamically interesting. We may not be able to predict which solution has interesting physical properties when studying more general actions. A solution that is not interesting in the canonical case might be of special interest when the action is generalized. Therefore, we emphasize the importance of having a thorough procedure for finding all valid solutions.

Having the Hubble parameter, we can derive the field and potential using equations (2.7) and (2.8). For (2.13) case we get

$$\phi(N) = \pm \sqrt{-\frac{2}{\beta}} \operatorname{arcsinh}\left(e^{\beta N}\right) + \phi_c, \quad (2.16)$$

$$V(\phi) = M^2 \left[ 3 + (\beta + 3) \sinh^2 \left( \sqrt{-\frac{\beta}{2}} (\phi - \phi_c) \right) \right], \quad (2.17)$$

$$\ddot{a}(N) = aM^2 \left( 1 + (\beta + 1)e^{2\beta N} \right), \quad (2.18)$$

where  $\phi_c$  is a constant of integration, and in (2.18) we have used the relation  $da/dN = a$ . Let us now check whether this solution describes a viable inflationary period. First of all, the parameters  $H$ ,  $V$ ,  $\phi$  must be real. For this condition to be satisfied, the constant-roll parameter  $\beta$  should be negative (since the field (2.16) is imaginary for  $\beta > 0$ ). According to equation (2.8), for a real  $\phi_{,N}$ ,  $H_{,N}$  must be negative, which occurs when  $\epsilon_1$  is positive. Next, we note that inflation is a period of positive acceleration. For acceleration to be positive  $\epsilon_1$  must be smaller than 1 (this point is easy to understand when one writes  $\ddot{a} = aH^2(1 - \epsilon_1)$ ). Lastly, we discuss the potential sign. Using equations (2.1), (2.3), and (2.4), potential can be written as  $V/H^2 = 3 - \epsilon_1$ . From this we notice that the potential is positive unless  $\epsilon_1$  exceeds 3. But this never happens because inflation already ends when  $\epsilon_1$  exceeds 1. Putting these together, we conclude that condition  $0 < \epsilon_1 < 1$  is required during inflation. After substituting the Hubble parameter (2.13) into equations (2.4), the slow-roll parameters can be derived as follows:

$$\epsilon_1(N) = \frac{-\beta}{1 + e^{-2\beta N}}, \quad \epsilon_{2j}(N) = \frac{2\beta}{1 + e^{2\beta N}}, \quad \epsilon_{2j+1}(N) = 2\epsilon_1(N), \quad (2.19)$$

where  $j$  is a positive integer. Slow-roll parameters (2.19) are illustrated in the top left panel of Figure 1. In large negative  $N$ , the first slow-roll parameter can be approximated as  $\epsilon_1 \approx -\beta$ , and in large positive  $N$  it tends to zero. That means for  $-1 < \beta < 0$  condition  $0 < \epsilon_1 < 1$  is always satisfied. However, for  $\beta < -1$ ,  $\epsilon_1$  is smaller than 1 only when  $2\beta N < \ln(-1/(\beta + 1))$ . Moreover, it is clear that  $\beta$  cannot be positive as it leads to negative  $\epsilon_1$ . Consequently, inflation conditions are met when  $-1 \leq \beta < 0$ , or when  $\beta < -1$  and  $2\beta N < \ln(-1/(\beta + 1))$ .

Similarly we can discuss the acceptable ranges for solutions (2.14) and (2.15). For (2.14)

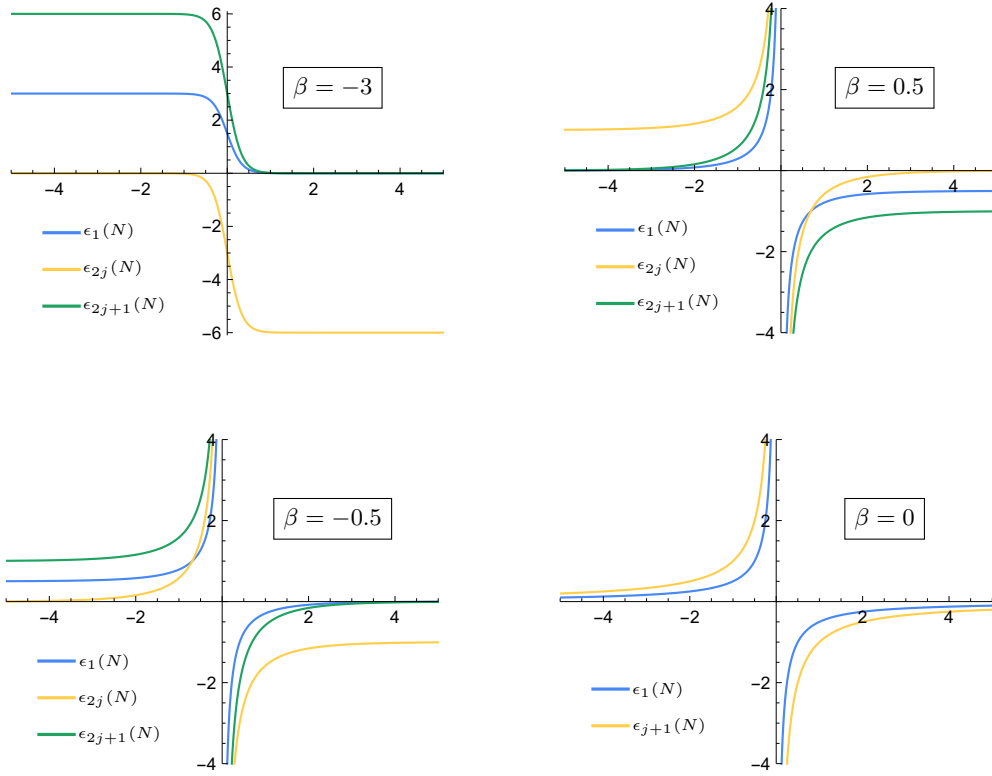


**Figure 1.** Slow-roll parameters for the canonical constant-roll model. Parameters (2.19), (2.23), (2.27), and (2.34) are plotted in the top left, top right, bottom left, and bottom right panels respectively.

case we can find

$$\phi(N) = \pm \sqrt{\frac{2}{\beta}} \arccos(e^{\beta N}) + \phi_c, \quad (2.20)$$

$$V(\phi) = M^2 \left[ 3 - (\beta + 3) \cos^2 \left( \sqrt{\frac{\beta}{2}} (\phi - \phi_c) \right) \right], \quad (2.21)$$

$$\ddot{a}(N) = aM^2 \left( 1 - (\beta + 1)e^{2\beta N} \right). \quad (2.22)$$

And the slow-roll parameters are

$$\epsilon_1(N) = \frac{-\beta}{1 - e^{-2\beta N}}, \quad \epsilon_{2j}(N) = \frac{2\beta}{1 - e^{2\beta N}}, \quad \epsilon_{2j+1}(N) = 2\epsilon_1(N). \quad (2.23)$$

Figure 1 (top right panel) shows these parameters for  $\beta = 0.5$ . In this case,  $\epsilon_1$  is positive and Hubble parameter is real only if  $N < 0$  and  $\beta > 0$ . At  $N = 0$ , however,  $\epsilon_1$  is singular and moves to infinity. Therefore, for the condition  $\epsilon_1 < 1$  to be satisfied,  $2\beta N$  must remain

smaller than  $\ln(1/(\beta + 1))$ . For (2.15) case we get

$$\phi(N) = \pm \sqrt{-\frac{2}{\beta}} \operatorname{arccosh}\left(e^{\beta N}\right) + \phi_c, \quad (2.24)$$

$$V(\phi) = M^2 \left[ (\beta + 3) \cosh^2 \left( \sqrt{-\frac{\beta}{2}} (\phi - \phi_c) \right) - 3 \right], \quad (2.25)$$

$$\ddot{a}(N) = aM^2 \left( (\beta + 1)e^{2\beta N} - 1 \right), \quad (2.26)$$

and for slow-roll parameters we have

$$\epsilon_1(N) = \frac{-\beta}{1 - e^{-2\beta N}}, \quad \epsilon_{2j}(N) = \frac{2\beta}{1 - e^{2\beta N}}, \quad \epsilon_{2j+1}(N) = 2\epsilon_1(N). \quad (2.27)$$

These parameters are plotted in Figure 1 (bottom left panel) for  $\beta = -0.5$ . Here  $\epsilon_1$  is positive and Hubble parameter is real only if  $N < 0$  and  $\beta < 0$ . At large negative  $N$  we can approximate  $\epsilon_1$  to  $-\beta$ . In this limit condition  $0 < \epsilon_1 < 1$  leads to  $-1 < \beta < 0$ . On the other hand, when  $N \rightarrow 0$ ,  $\epsilon_1$  moves to infinity, and condition  $2\beta N > \ln(1/(\beta + 1))$  is required to keep  $\epsilon_1$  smaller than 1.

It is noteworthy that  $\beta = -3$  is not allowed in potentials (2.21) and (2.25), whereas it is allowed in potential (2.17). It follows that only potential (2.17) can represent a case of USR inflation.

Heretofore we were able to find all possible constant-roll solutions analytically. However, our solutions are singular at  $\beta = 0$  (see equations (2.16), (2.20), and (2.24)). We can also see the singularity by setting  $\beta = 0$  in equations (2.13), (2.14), and (2.15). This results in the trivial solution  $H = \text{constant}$  with  $\epsilon_1 = 0$  and a singular  $\epsilon_2$ . To examine the model at this point, we integrate the constant-roll condition (2.10) again, this time by setting  $\beta$  to zero. We will find

$$H^2 = C(N - N_0), \quad (2.28)$$

where  $C$  and  $N_0$  are in general two complex numbers. Taking into account that the Hubble parameter is real, we are left with the following choices:

$$H^2 = -M^2 N, \quad (2.29)$$

$$H^2 = +M^2 N, \quad (2.30)$$

where,  $M^2 = |C|$  and without losing generality we have set  $N_0$  to zero. We first note that solution (2.30) is not acceptable as it leads to a positive  $H_{,N}$  and an imaginary  $\phi_{,N}$ . For solution (2.29) the field, potential, and acceleration are as follows:

$$\phi(N) = \pm 2\sqrt{-N} + \phi_c, \quad (2.31)$$

$$V(\phi) = \frac{1}{4}M^2 \left[ 3(\phi - \phi_c)^2 - 2 \right], \quad (2.32)$$

$$\ddot{a}(N) = -\frac{1}{2}aM^2(1 + 2N), \quad (2.33)$$

and for the slow-roll parameters we get

$$\epsilon_1(N) = -\frac{1}{2N}, \quad \epsilon_{j+1}(N) = 2\epsilon_1(N). \quad (2.34)$$

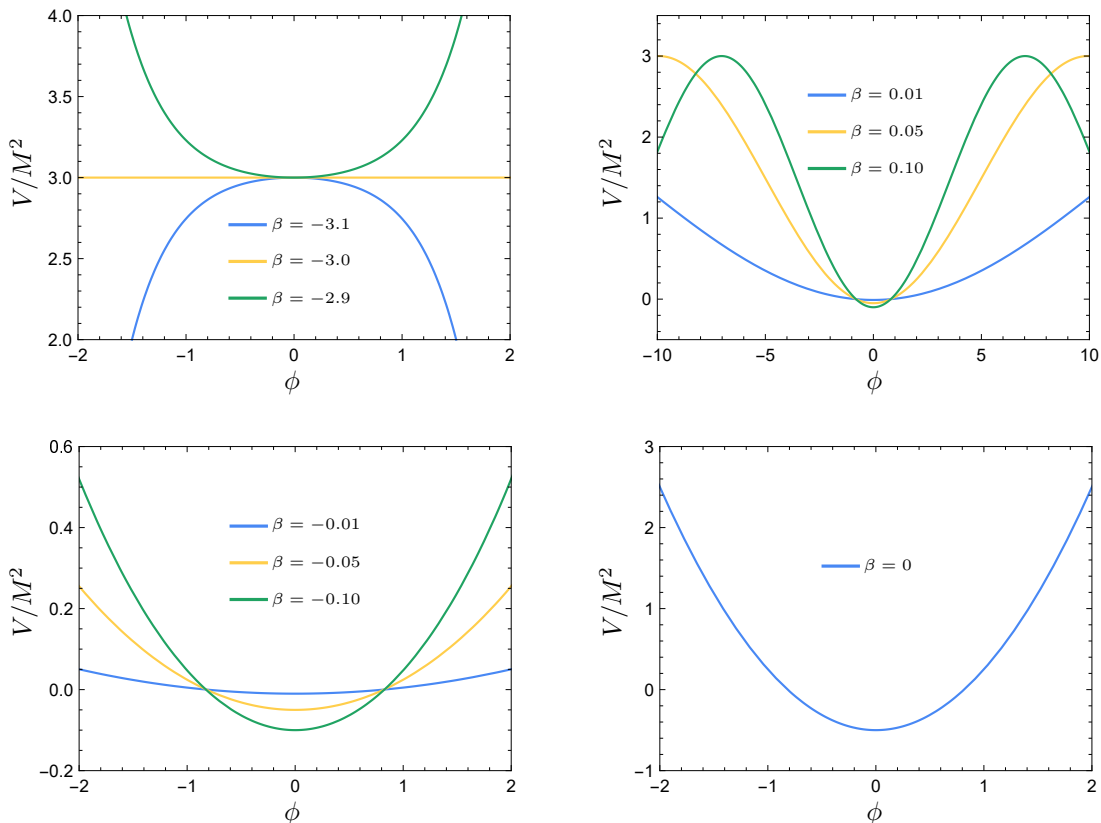


**Figure 2.** The class of canonical constant-roll potentials. Potentials (2.17), (2.21), (2.25), and (2.32) are plotted in the top left, top right, bottom left, and bottom right panels respectively. The parameter  $\phi_c$  is set to zero in all plots.

The slow-roll parameters (2.34) are plotted in the bottom right panel of Figure 1. In this case inflation conditions are satisfied for  $N < -1/2$ .

With this last solution, we have completely discussed the dynamics of the canonical constant-roll model. We presented our solutions as a functions of  $N$  simply because we found it more convenient. Solutions (2.13) and (2.14) correspond to the two cases studied in reference [12], and solution (2.15) corresponds to the special case studied in reference [13]. To our knowledge solution (2.29) has not been discussed previously (probably because it is transient and not dynamically interesting, which we will discuss later).

Figure 2 shows all constant-roll potentials (2.17), (2.21), (2.25), and (2.32). As can be seen, the potentials are extremely flat for  $\beta \rightarrow -3$  (USR limit) and  $\beta \rightarrow 0$  (slow-roll limit). But when  $\beta$  is exactly zero, the potential has a parabolic shape. It is true that in the case of the slow-roll, as in the case of USR, the potential should be very flat to ensure a slow rate of roll and a minimum of 40-60 e-folds of inflation. But if one defines USR as a model with a flat potential, then  $\beta \rightarrow 0$  is also an USR case, and there is no clear distinction between USR and slow-roll models. Therefore, in order to avoid ambiguities, we define USR limit with condition  $V_{,\phi} \ll \{\dot{\phi}, \ddot{\phi}\}$ , and slow-roll limit with  $\{\epsilon_1, \epsilon_2, \dots\} \ll 1$  (which in the canonical case leads to  $\ddot{\phi} \ll \dot{\phi} \ll 1$ ). This definition still allows for a model that is both USR and slow-roll (for  $V_{,\phi} \ll \ddot{\phi} \ll \dot{\phi} \ll 1$ ). But by expanding the potential and field for solutions (2.13), (2.14), and (2.15), around 0 and  $-3$ , we find that for  $\beta \rightarrow 0$  we have  $V_{,\phi}/\ddot{\phi} \propto 1/\beta$ , while for  $\beta \rightarrow -3$

we have  $V_{,\phi}/\ddot{\phi} \propto \beta + 3$  and  $V_{,\phi}/\dot{\phi} \propto \beta + 3$ . Thus,  $\beta \rightarrow 0$  does not represent an USR case but  $\beta \rightarrow -3$  does. Solution (2.29) also is not an USR case as it leads to  $\ddot{\phi} = 0$  and condition  $V_{,\phi} \ll \ddot{\phi}$  cannot be satisfied.

It could also be argued that the name "USR" is inappropriate. Because USR begins with a period of fast roll inflation. Nevertheless, we do not obsess over nomenclature in this work and respect the names that have long been used.

Additionally, it should be noted that all USR cases cannot be explained by constant-roll condition (2.6). In other words, any potential that is extremely flat might be considered an USR potential, and not only the constant-roll potentials described in equation (2.17). Therefore, by setting  $\beta \approx -3$ , we are examining only a particular set of potentials from a broader class of USR potentials. A similar argument can be made for the slow-roll limit  $\beta \approx 0$ . In the slow-roll approximation  $\ddot{\phi}/H\dot{\phi}$  is very small and not necessarily constant.

Our next step is to evaluate the spectral index and the non-Gaussianity parameter in order to examine the behavior of perturbations. In solution (2.13) at large positive  $N$  and solution (2.14) at large negative  $N$ ,  $\epsilon_1$  and  $\epsilon_3$  are small and  $\epsilon_2$  is roughly  $2\beta$ . Therefore, the spectral index can be approximated as (see Appendix A)

$$n_s - 1 = \begin{cases} 2(\beta + 3), & \beta < -3/2 \\ -2\beta, & \beta \geq -3/2 \text{ and } \beta \neq 0 \end{cases}. \quad (2.35)$$

The 2018 Planck data [74] constrain the spectral index as  $n_s = 0.9649 \pm 0.0042$ . Accordingly, the only feasible values for the constant-roll parameter are  $\beta \approx 0.018$  and  $\beta \approx -3.018$ . It is imperative to note that the power (2.35) is evaluated at horizon exit. However, as we will show later, in the case  $\beta < -3/2$  the modes continue to grow on the superhorizon scales and the effect of growing modes should also be taken into account in the evaluation of the power spectrum. Consequently, for  $\beta \approx -3.018$ , result (2.35) is invalid, and  $\beta \approx 0.018$  is the only compatible point.

In solutions (2.13) and (2.15) if inflation starts at large negative  $N$  we have  $\epsilon_1 \approx -\beta$  and  $\epsilon_3 \approx -2\beta$  while  $\epsilon_2$  is small. So for spectral index we get [75]

$$n_s - 1 = \frac{2\beta}{\beta + 1}. \quad (2.36)$$

In this case, the constant-roll parameter is constrained to  $\beta \approx -0.017$ , based on Planck data. Finally, for solution (2.29), since all slow-roll parameters are small, we will have the following spectral index:

$$n_s - 1 = -4\epsilon_1. \quad (2.37)$$

To agree with the Planck data,  $\epsilon_1$  should be in the range of 0.0077 to 0.0098, which is between  $N = -65$  and  $-51$ . That means this case is transient and can last up to 14 e-folds. As far as we know, results (2.36) and (2.37) are new.

To determine whether our solutions are attractor and stable, we plot the phase space diagrams. For the first solution (2.16), phase space is illustrated Figure 3 (left panel). This picture clearly shows that the constant-roll trajectory for  $\beta = -2.5$  (green line) is not an attractor, but its corresponding dual constant-roll solution is. Dual solutions are constant-roll solutions for  $\tilde{\beta} \approx -3 - \beta$ . References [14, 15] provide more information about the duality of constant-roll solutions.

In Figure 3, the middle and right panels illustrate phase space diagrams for solutions (2.20) and (2.24). As can be seen, these solutions are attractor and stable.

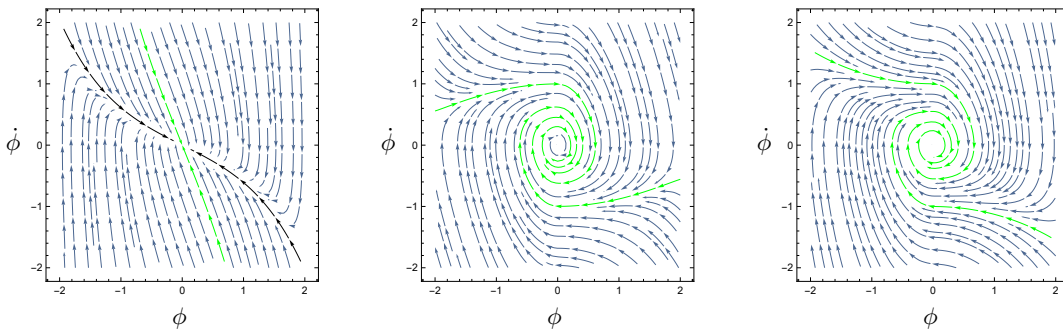


**Figure 3.** Left, middle, and right panels show phase portrait diagrams for canonical constant-roll solutions (2.16) (for  $\beta = -2.5$ ), (2.20) (for  $\beta = 0.5$ ), and (2.24) (for  $\beta = -0.5$ ). Green lines are unperturbed constant-roll trajectories. The black line in the left panel shows the corresponding dual constant-roll trajectory,  $\beta \approx -0.5$ .

For solution (2.31),  $\beta$  is taken to be exactly zero. In this case, a slight change in initial values (that changes  $\beta$ ) will result in switching to another constant-roll solution and never returning to  $\beta = 0$  again. As a result, this solution is also unstable. In general, all  $\beta < -3/2$  solutions are unstable, while all  $\beta \geq -3/2$  solutions, except for  $\beta = 0$ , are stable.

This work does not focus on studying non-Gaussianity. However, the non-Gaussian properties of solution (2.13) are particularly interesting and worth discussion. In this case the contribution due to the field redefinition to the non-Gaussianity can be derived as follows (see Appendix A):

$$f_{NL}^{re} = \begin{cases} -\frac{5}{2}(\beta + 2) = \frac{5}{4}(3 - n_s), & \beta < -3/2 \\ \frac{5}{6}\beta = \frac{5}{12}(1 - n_s), & \beta \geq -3/2 \text{ and } \beta \neq 0 \end{cases}. \quad (2.38)$$

Parameter (2.38) is of order one for  $\beta \approx -3.018$  and contributes the most to non-Gaussianity. However, when  $\beta \approx 0.018$ , this parameter is of order one for the slow-roll parameter and its contribution to non-Gaussianity is comparable to some terms in the action. Additionally, Maldacena's consistency relation [76] is satisfied for  $\beta \approx 0.018$ , but violated for  $\beta \approx -3.018$ .

A look at the evolution of curvature perturbations on super Hubble scales ( $k \ll aH$ ) can help explain the sudden change of behavior in equations (2.35) and (2.38) at  $\beta = -3/2$ . The  $k^2$  term in the Mukhanov-Sasaki equation (A.2) is negligible at super Hubble scales. As a result, we can integrate this equation to get [10]:

$$u = C_1 + C_2 \int \frac{d\tau}{a^2 \epsilon_1} = C_1 + \frac{C_2}{a_0^3 H} \int \frac{dN}{e^{3N} \epsilon_1}, \quad (2.39)$$

where  $C_1$  and  $C_2$  are two arbitrary constants, and for the last equality we have used the relation  $a = a_0 \exp(N)$  (derived by integrating the definition  $dN \equiv d \ln a$ ), as well as the fact that Hubble parameter is roughly constant at large scales. As can be seen in equation (2.39), the curvature perturbation has a constant part and an integral part. If  $\epsilon_1$  is decaying slower than  $e^{-3N}$ , then the mode function will converge to a constant at super Hubble scales. In contrast, when  $\epsilon_1$  decays faster than  $e^{-3N}$ , the integral part diverges and the mode function continues to evolve at large scales. Consistency relation requires that the long modes are well frozen out at large scales, which is not the case here. Therefore, Maldacena's methodology for proving non-Gaussianity is small does not apply here, and consistency relation cannot be

satisfied for fast decaying  $\epsilon_1$ . In equation (2.19), it is evident that for  $\beta = -3/2$ , the slow-roll parameter decays as  $e^{-3N}$ . This completely explains why equations (2.35) and (2.38) suddenly change their behavior at  $\beta = -3/2$ .

### 3 Constant-Roll Condition in Non-Canonical Models

In previous section, the constant-roll condition was defined by three equivalent expressions given in (2.6). In this section, we consider each expression as a distinct constant-roll condition and impose it on a general  $P(X)$  model to show that the nature of the model and its consequences is sensitive to the expression we use. Furthermore, the equivalence is restricted to some models, like single field canonical case, and the result would be different for either expression, in other inflationary models.

A general  $P(X)$  model is described by the following action,

$$S = \frac{1}{2} \int d^4x \sqrt{-g} [R + 2P(X, \phi)]. \quad (3.1)$$

In FLRW background with  $(-, +, +, +)$  signature,  $X = \dot{\phi}^2/2$  corresponds to the canonical kinetic term. The Friedman equations for this action are

$$3H^2 = 2XP_{,X} - P, \quad (3.2)$$

$$\dot{H} + XP_{,X} = 0. \quad (3.3)$$

The time evolution of the homogenous mode of the field  $\phi(t)$  is governed by the Klein-Gordon equation

$$\ddot{\phi} + 3c_s^2 H \dot{\phi} + \mathcal{V}_{,\phi} = 0. \quad (3.4)$$

Here  $c_s$  represents the sound speed which can be expressed as

$$c_s^2 = \frac{P_{,X}}{P_{,X} + 2XP_{,XX}}, \quad (3.5)$$

and the non-trivial field dynamics is controlled by the friction term and an effective potential given by

$$\mathcal{V}_{,\phi} = \frac{c_s^2 \left( \dot{\phi}^2 P_{,X\phi} - P_{,\phi} \right)}{P_{,X}}. \quad (3.6)$$

In our first approach to add a constant-roll condition to the above system of equations, we consider the conventional form given by

$$\frac{\ddot{\phi}}{H\dot{\phi}} = \beta_F, \quad (3.7)$$

where subscript F refers to a constant-roll condition that constraints the field rate of roll. We call this constraint the *field-constant-roll* (FCR) condition. This constant-roll condition can be written as  $d \ln \dot{\phi} / dN = \beta_F$ , indicating that the scalar field has a constant roll rate. Integrating it out, we find

$$\dot{\phi} \propto e^{\beta_F N}. \quad (3.8)$$

This relation indicates that  $|\dot{\phi}|$  grows (decays) rapidly for  $\beta_F > 0$  ( $\beta_F < 0$ ). Note that this behavior is simply a consequence of the FCR condition and has been derived regardless of the form of the action.

As the second approach, we define a constant-roll condition that (similar to the canonical case) leads to a constant  $\epsilon_2$ . Provided that the first slow-roll parameter is small<sup>2</sup>, then the second slow-roll parameter  $\epsilon_2 = 2\epsilon_1 + \ddot{H}/(H\dot{H})$  is roughly constant by imposing the following condition:

$$\frac{\ddot{H}}{2H\dot{H}} = \beta_{\text{H}}. \quad (3.9)$$

We refer to this constraint as the *Hubble-constant-roll* (HCR) condition. Note that, unlike the canonical case,  $\beta_{\text{H}}$  here does not always equal to  $\ddot{\phi}/(H\dot{\phi})$ . The HCR condition does not ensure a constant rate of roll for the scalar field. Likewise, the FCR condition does not guarantee a constant  $\epsilon_2$ .

An interesting property of the HCR condition is that we can directly integrate it to obtain the Hubble parameters given by (2.13), (2.14), (2.15), and (2.29). Accordingly, the slow-roll parameters and the acceptable ranges for  $N$  and  $\beta_{\text{H}}$  are also similar to the canonical case.

To see how FCR and HCR conditions are interconnected and whether the latter can also be interpreted as a constant rate of roll, let us find the relation between what we call  $\beta_{\text{F}}$  and  $\beta_{\text{H}}$ . We use equation (3.3) to write the FCR condition (3.7) as

$$\frac{\ddot{H}}{H\dot{H}} = \frac{\dot{\phi} Q_{,X\phi}}{HQ_{,X}} + \left( \frac{c_s^2 + 1}{c_s^2} \right) \beta_{\text{F}}, \quad (3.10)$$

where we have defined the effective kinetic term,  $Q(X, \phi) \equiv P(X, \phi) + V(\phi)$ . From this we notice that when the FCR condition is imposed,  $\ddot{H}/(H\dot{H})$  is not necessarily constant. In a particular model, if the right hand side of equation (3.10) becomes constant, the HCR condition is met. In this case we can use (3.9) to rewrite (3.10) as

$$2\beta_{\text{H}} = \frac{\dot{\phi} Q_{,X\phi}}{HQ_{,X}} + \left( \frac{c_s^2 + 1}{c_s^2} \right) \beta_{\text{F}}. \quad (3.11)$$

With fixed  $P(X, \phi)$ , for the models constrained with FCR and HCR conditions to be homologous, the condition (3.11) must be satisfied. Canonical constant-roll model satisfies this relation for  $\beta_{\text{F}} = \beta_{\text{H}}$ .

A key property of the canonical constant-roll model is that it leads to USR for  $\beta \rightarrow -3$ , and it can be considered a generalization of USR model. However, our FCR and HCR conditions do not always correspond to the generalization of USR. In other words, in a particular model, these constant-roll conditions may not reduce to a flat USR potential for any choice of the constant-roll parameter. As our final approach to the generalized constant-roll condition, we define the constant-roll conditions so that the profile of the scalar potential  $V(\phi)$  is sufficiently flat when constant-roll parameter approaches  $-3$ . We approximate the field equation (3.4) in the USR limit as

$$V_{,\phi} \ll \{\dot{\phi}, \ddot{\phi}\} \quad \Rightarrow \quad \ddot{\phi} + 3c_s^2 H \dot{\phi} + \frac{c_s^2 (\dot{\phi}^2 Q_{,X\phi} - Q_{,\phi})}{Q_{,X}} = 0. \quad (3.12)$$

According to this equation, we define our third constant-roll condition as

$$\frac{\ddot{\phi}}{H\dot{\phi}} = c_s^2 \beta_{\text{V}} - \frac{c_s^2 (\dot{\phi}^2 Q_{,X\phi} - Q_{,\phi})}{H\dot{\phi} Q_{,X}}, \quad (3.13)$$

---

<sup>2</sup>This is usual in the standard models of inflation based on an inflationary attractor dynamics.

and refer to this constraint as the *potential-constant-roll* (PCR) condition. Non-canonical models constrained by (3.13) are generalizations of USR, in the sense that they lead to a flat potential when  $\beta_V$  approaches  $-3$ . One may use equation (3.4) to rewrite the PCR condition (3.13) in the familiar form

$$\dot{V} = 2H\dot{H}(3 + \beta_V). \quad (3.14)$$

Although our third manipulation of constant-roll constraint makes implicit use of the third expression in (2.6), it is important to emphasize that condition (3.14) is not the only possible way to generalize the USR. For instance, the condition  $\dot{V} = (3 + \beta_V)HV$ , which again exhibits USR when  $\beta_V \rightarrow -3$  can be viewed as another generalization of USR and may provide new insights into the model. Nevertheless, the form (3.14) has two advantages: it is identical to FCR and HCR conditions in the canonical limit, and for the examples we will discuss later,  $\beta_V \rightarrow 0$  leads to slow-roll case. In this work, we discuss only a small number of an apparently endless variety of possible constant-roll conditions picked out by the demand of having canonical counterpart.

One can also derive the relation between  $\beta_V$  and  $\beta_F$  by utilizing definitions (3.7) and (3.13)

$$\beta_F = c_s^2 \beta_V - \frac{c_s^2 (\dot{\phi}^2 Q_{,X\phi} - Q_{\phi})}{H\dot{\phi} Q_{,X}}. \quad (3.15)$$

To find the relation between  $\beta_V$  and  $\beta_H$ , we elaborate on equation (3.3) to rewrite the PCR condition as

$$\frac{\ddot{H}}{H\dot{H}} = (1 + c_s^2) \beta_V + \frac{(c_s^2 + 1) Q_{,\phi} - c_s^2 \dot{\phi}^2 Q_{,X\phi}}{H\dot{\phi} Q_{,X}}. \quad (3.16)$$

This implies that given a non-canonical action, two constant-roll models based on PCR and HCR constraint would be homologous if we have

$$2\beta_H = (1 + c_s^2) \beta_V + \frac{(c_s^2 + 1) Q_{,\phi} - c_s^2 \dot{\phi}^2 Q_{,X\phi}}{H\dot{\phi} Q_{,X}}. \quad (3.17)$$

Finally, note that the system of equations (3.11), (3.15), and (3.17) are dependent, in the sense that when every pair of the equations are satisfied, all three kinds of constant-roll conditions lead to similar results. The canonical constant-roll model satisfies these conditions for  $\beta_F = \beta_H = \beta_V$ . In what comes next, we arrange to clearly distinguish between the above approaches for generalizing the constant-roll conditions.

## 4 Constant-Roll and Propagation Inflation

This section considers a special class of inflationary models with constant sound speed to demonstrate the applications of the constant-roll conditions discussed in section 3. With constant  $c_s$ , integration of equation (3.5) gives us

$$P(X, \phi) = \mathcal{F}(\phi)X^\lambda - V(\phi), \quad (4.1)$$

where  $\mathcal{F}(\phi)$  and  $V(\phi)$  are two arbitrary functions of  $\phi$ , and for simplicity we have defined  $\lambda \equiv XP_{,XX}/P_{,X} + 1 = (c_s^2 + 1)/(2c_s^2) \geq 1$ . We refer to this class of models as *constant propagation inflation*. By imposing the constant-roll condition on the model in the following subsections, we will have a class of *constant-roll and propagation inflation*. In the case of

$c_s = 1$ , the constant propagation model (4.1) takes the form  $P(X, \phi) = \mathcal{F}X - V$ , also known as k/G inflation [67].

Using relation (4.1) the dynamics of these models is governed by

$$3H^2 = \frac{\mathcal{F}}{c_s^2} X^\lambda + V, \quad (4.2)$$

$$\dot{H} + \lambda \mathcal{F} X^\lambda = 0, \quad (4.3)$$

$$\ddot{\phi} + 3c_s^2 H \dot{\phi} + \mathcal{V}_{,\phi} = 0, \quad (4.4)$$

where derivative of effective potential is given by

$$\mathcal{V}_{,\phi} = \frac{X \mathcal{F}_{,\phi}}{\lambda \mathcal{F}} + \frac{c_s^2 V_{,\phi}}{\lambda \mathcal{F}} X^{1-\lambda}. \quad (4.5)$$

For  $c_s = \mathcal{F} = 1$ , we can verify that the general argument presented here leads to the canonical case discussed in section 2.

In this section we study three classes of constant-roll and propagation models constrained with constant-roll conditions introduced in previous section. However, before proceeding, it is useful to determine whether these classes would be homologous or not. The effective kinetic term in constant propagation model is given by

$$Q = P + V = \mathcal{F}X^\lambda. \quad (4.6)$$

Using this, we can show that constant propagation models satisfy equation (3.17) with  $2\beta_H = (1 + c_s^2) \beta_V$ . In other words, in a constant propagation model if  $\beta_H$  is constant,  $\beta_V$  is also constant and vice versa. Therefore, HCR and PCR constrained classes are not independent and do not lead to different solutions. By knowing that, we can easily discuss the model's USR limit. Since for HCR condition the Hubble parameter can be derived identical to the canonical case, and since in the constant propagation model the HCR and PCR condition are homologous, the Hubble parameter and slow-roll parameters in USR case of the constant propagation models are given by equations (2.13) and (2.19), but with  $\beta$  replaced with  $-3(c_s^2 + 1)/2$ . As we discussed in section 2, if  $\epsilon_1$  decays faster than  $e^{-3N}$  modes keep growing at superhorizon scales. Thus, the model cannot be stable unless the condition  $\beta = -3(c_s^2 + 1)/2 > -3/2$  or equivalently  $c_s^2 < 0$  is satisfied, which is impossible. It follows that the USR limit of constant propagation model (4.1) can never be stable.

Using (4.6) again, we can write equation (3.11) as

$$\beta_H = \frac{\dot{\mathcal{F}}}{2H\mathcal{F}} + \lambda\beta_F. \quad (4.7)$$

This means that FCR and HCR constrained classes are generally independent and lead to different solutions unless the offending non-universal term  $\dot{\mathcal{F}}/(2H\mathcal{F})$  is a constant.

#### 4.1 Field-Constant-Roll Condition

We now discuss the dynamics of the constant propagation class (4.1) constrained with the FCR condition (3.7). In this case, if  $\mathcal{F}(\phi)$  is known, one can start the study by integrating the constant-roll condition (3.7) written in the following form:

$$\beta_F = \frac{c_s^2}{H} \left[ -\frac{2^\lambda H_{,\phi}}{\lambda \mathcal{F}} \right]^{c_s^2} \left( \ln \frac{H_{,\phi}}{\mathcal{F}} \right)_{,\phi}, \quad (4.8)$$

where equation (4.3) is implemented. Having  $\mathcal{F}(\phi)$ , one can solve this equation to find  $H(\phi)$ . Once Hubble parameter has been determined, the field velocity can be derived using equation (4.3) as follows:

$$\dot{\phi} = \left[ -\frac{2^\lambda H_{,\phi}}{\lambda \mathcal{F}} \right]^{c_s^2}, \quad (4.9)$$

and utilizing equation (4.2) for the potential we easily find

$$V = 3H^2 + \frac{H_{,\phi}}{\lambda c_s^2} \left[ -\frac{2^\lambda H_{,\phi}}{\lambda \mathcal{F}} \right]^{c_s^2}. \quad (4.10)$$

With the help of equations (3.7) and (4.3), for the first and second derivatives of effective potential we obtain

$$\mathcal{V}_{,\phi} = -(3c_s^2 + \beta_F)H\dot{\phi}, \quad (4.11)$$

$$\mathcal{V}_{,\phi\phi} = (3c_s^2 + \beta_F)(\epsilon_1 - \beta_F)H^2. \quad (4.12)$$

Note that, contrary to the potential expression (4.10), these relations are not directly dependent on  $\mathcal{F}$  function. It is clear from equation (4.11) that the derivative of effective potential vanishes at zeros of  $H$  and  $\dot{\phi}$ . On the other hand zeros of  $H_{,\phi}$  and  $\dot{\phi}$  coincide (see (4.9)) and we find the effective potential extremas at zeros of  $H$  and  $H_{,\phi}$ . Based on equation (4.12), we notice that, like the canonical case, at extrema the concavity of effective potential is determined by  $\beta_F$  values; the effective potential is concave for  $\beta_F < -3c_s^2$  and  $\beta_F > 0$ , and it is convex for  $-3c_s^2 < \beta_F < 0$ . For  $\beta_F = -3c_s^2$  the effective potential is flat.

Using general relation (3.8) and equation (4.3), for the number of  $e$ -folds we find

$$N - N_0 = \frac{c_s^2}{\beta_F} \ln \left( \frac{H_{,\phi}}{\mathcal{F}} \right), \quad (4.13)$$

We assume that  $H_{,\phi}$  has a zero at  $\phi = \tilde{\phi}$ . From equation (4.13) we notice that as  $\phi \rightarrow \tilde{\phi}$ , the expression  $\ln(H_{,\phi}/\mathcal{F})$  diverges and  $\beta_F(N - N_0)$  goes to negative infinity, if  $\mathcal{F}(\tilde{\phi}) \neq 0$ . Using equations (2.4), (4.3), and (4.13) we can find the following general relations for the first and second slow-roll parameters:

$$\epsilon_1 \propto \frac{\mathcal{F}}{H^2} e^{2\lambda\beta_F N}, \quad \epsilon_2 = 2\epsilon_1 + 2\lambda\beta_F + \frac{\dot{\mathcal{F}}}{H\mathcal{F}}. \quad (4.14)$$

As the scalar field starts to traverse the extrema of the effective potential at  $\phi = \tilde{\phi}$ ,  $\mathcal{F}(\phi)$  and  $H(\phi)$  approach the constant values of  $\mathcal{F}(\tilde{\phi})$  and  $H(\tilde{\phi})$  and we have an exponentially decreasing (increasing)  $\epsilon_1$  for positive (negative)  $\mathcal{F}(\tilde{\phi})$ . Furthermore, if the time scale of  $\mathcal{F}$  variation is large enough and  $\epsilon_1$  is sufficiently small, for the second slow-roll parameter we get  $\epsilon_2 \propto 2\lambda\beta_F$ . Therefore, the model exhibits a *quasi-canonical* behavior as  $\phi \rightarrow \tilde{\phi}$  (and if we have  $\mathcal{F}(\tilde{\phi}) = 1$ , then we will observe normal canonical behavior). if this phase is characterized by a large negative  $\tilde{\beta}_F \equiv \lambda\beta_F < -3/2$ , its dynamics enter the non-attractor era lasting some  $e$ -folds of evolution during which the first slow-roll parameter decays exponentially.

The solutions with  $\beta_F < -3c_s^2$  and  $\beta > 0$  are of phenomenological interest. In this case the scalar field rolls up a bump-like region and asymptotically comes to rest at the top of the bump. This will be the case for the fine-tuned initial condition and these constant-roll solutions lead classically to eternal inflation. Under quantum perturbations, however, this

will be a transient solution. As we will show in an example in section 4.3, the generic attractor solution is the dual case  $\beta_F \rightarrow -(\beta_F + 3c_s^2)$ . The transition from the smaller  $\beta_F$  to the larger value  $-(\beta_F + 3c_s^2)$  can be seen through the Klein-Gordon equation (4.4) linearized around the maximum of the effective potential,

$$\ddot{\phi} + 3c_s^2 H(\tilde{\phi}) \dot{\phi} - \beta_F (\beta_F + 3c_s^2) H^2(\tilde{\phi}) (\phi - \tilde{\phi}) \approx 0. \quad (4.15)$$

which is invariant under the duality transform. By utilizing (4.11), an equivalent definition of  $\beta_F$  is given by  $\beta_F = -3c_s^2 + \mathcal{V}_{,\phi}/(H\dot{\phi})$ . This form indicates that (if the field velocity is large enough so that the field can pass the extrema), when the field evolves through the critical point  $\phi = \tilde{\phi}$ , the parameter  $\beta_F$  is forced to  $-3c_s^2$ . The value of  $-3c_s^2$  for the  $\beta_F$  at the maximum of the effective potential is a feature of FCR condition, and as we will show later, it will depend on the  $\mathcal{F}$  profile in the HCR (and equivalently PCR) models.

## 4.2 Hubble-Constant-Roll and Potential-Constant-Roll Conditions

We discussed that in the constant propagation class (4.1) the HCR and PCR conditions are analogous. Therefore, we only consider HCR conditions (3.9) here. We know that the Hubble parameter in these models are similar to the canonical case. Accordingly, the first and second slow-roll parameters are given by

$$\epsilon_1 \propto \frac{1}{H^2} e^{2\beta_H N}, \quad \epsilon_2 = 2\epsilon_1 + 2\beta_H. \quad (4.16)$$

We observe that in general, slow-roll parameters here differ from (4.14) parameters derived using the FCR condition. However, at the critical point  $\tilde{\phi}$ , both HCR and FCR constrained models exhibit an approximately identical quasi-canonical behavior with  $\beta_H = \tilde{\beta}_F = \lambda\beta_F$ . Indeed, this is well consistent with our previous general argument that in constant propagation models three constant-roll conditions are homologous when the timescale of  $\mathcal{F}$  variation is large (see equation (4.7)).

After removing  $\mathcal{F}$  between equations (4.2) and (4.3), we will have

$$V = 3H^2 + \frac{2\dot{H}}{c_s^2 + 1}. \quad (4.17)$$

In this equation, we can write the time derivative in terms of  $N$  and use Hubble parameters (2.13), (2.14), (2.15), and (2.29) to find the following potentials respectively:

$$V(N) = M^2 \left[ 3 + \left( \frac{2\beta_H}{c_s^2 + 1} + 3 \right) e^{2\beta_H N} \right], \quad (4.18)$$

$$V(N) = M^2 \left[ 3 - \left( \frac{2\beta_H}{c_s^2 + 1} + 3 \right) e^{2\beta_H N} \right], \quad \beta_H > 0, \quad (4.19)$$

$$V(N) = M^2 \left[ \left( \frac{2\beta_H}{c_s^2 + 1} + 3 \right) e^{2\beta_H N} - 3 \right], \quad \beta_H < 0, \quad (4.20)$$

$$V(N) = M^2 \left[ 3N + \frac{1}{c_s^2 + 1} \right]. \quad (4.21)$$

The first three potentials are flat for  $\beta_H = 0$  and  $\beta_H = -3(c_s^2 + 1)/2$ . When  $\beta_H = 0$ , all slow-roll parameters are small, so this parameter value corresponds to a slow-roll case. By

the homologous relation mentioned above and described by  $2\beta_{\text{H}} = (c_s^2 + 1)\beta_{\text{V}}$ , the latter appears to be an USR case.

With Hubble parameter, potential, and slow-roll parameters in hand, we need to know the form of the parameter  $\mathcal{F}$  to find the dynamics of the inflaton field  $\phi(t)$  (or  $\phi(N)$ ). One can use equation (4.3) and its derivative to rewrite the constant-roll condition (3.9) as

$$\beta_{\text{H}} = \left[ \frac{-2^\lambda H_{,\phi}}{\lambda \mathcal{F}} \right]^{c_s^2} \left[ \frac{\lambda c_s^2}{H} \left( \ln \frac{H_{,\phi}}{F} \right)_{,\phi} + \frac{\mathcal{F}_{,\phi}}{2H\mathcal{F}} \right], \quad (4.22)$$

and integrating it out to find  $H(\phi)$ . The field is then calculated using the relation  $H(\phi) = H(t) = H(N)$ .

The effective potential gradient can be obtained from the general expression (3.6) and HCR condition (3.9) in the form of

$$\mathcal{V}_{,\phi} = c_s^2 H \dot{\phi} \left[ \frac{\dot{\mathcal{F}}}{2\lambda c_s^2 H \mathcal{F}} - (3 + \beta_{\text{V}}) \right]. \quad (4.23)$$

The effective potential has extrema at  $\phi = \tilde{\phi}$ , i.e, where  $\dot{\phi}$  or  $H$  vanishes. The expression for the second derivative of the effective potential is quite complex but at  $\phi = \tilde{\phi}$  it can be approximated as

$$\mathcal{V}_{,\phi\phi} \approx -c_s^4 H^2 \beta_{\text{V}} (3 + \beta_{\text{V}}). \quad (4.24)$$

It is clear that at the critical point  $\tilde{\phi}$ , where  $\mathcal{F}$  is roughly constant, expressions (4.23) and (4.24) become identical to those in the FCR constrained models, (4.11) and (4.12), with  $\beta_{\text{H}} = \lambda c_s^2 \beta_{\text{V}} = \lambda \beta_{\text{F}}$ . Therefore, based on our analysis, we expect to encounter the duality between  $\beta_{\text{H}}$  and  $-(\beta_{\text{H}} + 3\lambda c_s^2)$  solutions. Nevertheless, this discussion does not show that the model will actually transition to the dual solution. To determine whether  $\beta_{\text{H}}$  is parametrically forced to  $-(\beta_{\text{H}} + 3\lambda c_s^2)$ , we need to conduct a stability analysis that considers perturbations in the initial values of the model. We will perform such an analysis in the example provided in section 4.3. Indeed, approximation (4.15) only holds at the beginning and end of the transition trajectory, where the model approximately follows a constant-roll scenario. Hence, the transition trajectory cannot be accurately described by this approximation. The form of the transition trajectory generally depends on the specific form of the action. As a simple demonstration of this dependence, we can use equation (4.23) to express the constant-roll parameter as  $\beta_{\text{V}} = \dot{\mathcal{F}}/(2\lambda c_s^2 H \mathcal{F}) - \mathcal{V}_{,\phi}/(c_s^2 H \dot{\phi}) + 3$ . This relation highlights that the field velocity at the extrema of the effective potential, where  $\mathcal{V}_{,\phi} = 0$ , depends on the specific form of the parameter  $\mathcal{F}$  (unlike in the FCR case, where it is always equal to  $-3c_s^2$  irrespective of the form of the  $\mathcal{F}$  function).

Using general relations (3.9) and (4.3), number of  $e$ -folds and the field are related by

$$N - N_0 = \frac{1}{2\beta_{\text{H}}} \left[ 2\lambda c_s^2 \ln \left( \frac{H_{,\phi}}{\mathcal{F}} \right) + \ln \mathcal{F} \right]. \quad (4.25)$$

It is also worth noting that with constant  $c_s$  and slow-roll parameters similar to canonical models, the spectral index is also the same as the canonic (see Appendix A).

### 4.3 An Example: k/G Inflation

Having constructed the framework of constant-roll generalizations in constant propagation inflation, we will examine a particular example to demonstrate the mechanism discussed in

sections 4.1 and 4.2. We consider a subset of (4.1) as

$$P(X, \phi) = \mathcal{F}(\phi)X - V(\phi), \quad (4.26)$$

where we have chosen  $c_s = \lambda = 1$ . These models are well motivated and studied in [67]. For this reasoning, we found it interesting to study its application in constant-roll inflationary models. For  $c_s = 1$  general relations (4.8) and (4.22) become

$$\left(\frac{H, \phi}{\mathcal{F}}\right)_{, \phi} + \frac{\beta_{\text{F}}}{2}H = 0, \quad (4.27)$$

$$\left(\frac{H, \phi}{\sqrt{\mathcal{F}}}\right)_{, \phi} + \beta_{\text{H}}\sqrt{\mathcal{F}}H = 0. \quad (4.28)$$

We recall that these equations are the FCR and HCR conditions written in terms of derivatives with respect to the field. These equations are in the form of Sturm–Liouville equations with eigenvalues given by constant-roll parameters and orthogonal eigenfunctions with zeros at  $\phi = \tilde{\phi}$ . Note that in equation (4.28),  $\beta_{\text{H}}$  can be replaced by  $\beta_{\text{V}}$ . As we can see, the Hubble parameter  $H(\phi)$  is determined by the function  $\mathcal{F}(\phi)$ . For definiteness, we focus on a representative example,  $\mathcal{F} = \gamma\phi$ , and discuss its properties. Here,  $\gamma$  is a parameter with unit length dimension. With this choice, the following solutions are obtained for equations (4.27) and (4.28), respectively:

$$H(\phi) = C_1 Ai' \left( \sqrt[3]{-\frac{\gamma\beta_{\text{F}}}{2}\phi} \right) + C_2 Bi' \left( \sqrt[3]{-\frac{\gamma\beta_{\text{F}}}{2}\phi} \right), \quad (4.29)$$

$$H(\phi) = C_3 \cosh \left( \frac{1}{3} \sqrt{-2\gamma\beta_{\text{H}}\phi^3} \right) + C_4 \sinh \left( \frac{1}{3} \sqrt{-2\gamma\beta_{\text{H}}\phi^3} \right), \quad (4.30)$$

where  $C_i$ s are integration constants,  $Ai(z)$  and  $Bi(z)$  are Airy functions of the first and second kind, and prime denotes the derivative with respect to  $\phi$ .

Let us first examine the FCR solution (4.29). For convenience we consider a particular case with  $C_2 = 0$  as

$$H(\phi_{\text{F}}) = M Ai'(\phi_{\text{F}}), \quad (4.31)$$

where we have defined  $M \equiv C_1$ ,  $\bar{\beta}_{\text{F}} \equiv \sqrt[3]{-\beta_{\text{F}}\gamma/2}$ , and  $\phi_{\text{F}} \equiv \bar{\beta}_{\text{F}}\phi$ . A plot of the Hubble parameter (4.31) can be seen in Figure 4 (top left panel). To have a real Hubble parameter, we need to choose  $\gamma\beta_{\text{F}} < 0$ . As we wish to examine the model for both positive and negative  $\beta_{\text{F}}$ , we choose  $\beta_{\text{F}} = -0.5$  with  $\gamma = 1$ , as well as  $\beta_{\text{F}} = 0.5$  with  $\gamma = -1$ . These two cases share the same Hubble parameter but have different dynamics. Note that in our choices  $\bar{\beta}_{\text{F}}$  is positive and zeros of  $H, \phi \propto \phi_{\text{F}} Ai(\phi_{\text{F}})$  are located at  $\phi_{\text{F}} = 0$  and isolated values of  $\phi_{\text{F}}$  on negative real axis. Following the notation of reference [77], we show  $s^{\text{th}}$  zeros of  $Ai(z)$  and  $Ai'(z)$  with  $a_s$  and  $a'_s$ , respectively<sup>3</sup>. In particular, we will discuss the model around  $\phi_{\text{F}} = 0$  and  $\phi_{\text{F}} = a_1 \approx -2.34$  points where  $H, \phi$  becomes zero and we expect quasi-canonical behavior. It is important to note that at  $\phi_{\text{F}} = 0$  the Hubble parameter is negative, which means the universe is collapsing and is not acceptable. However, we can easily avoid this problem by choosing a negative  $M$ .

Having the Hubble parameter, we can use the general relation (4.13) to find the number  $e$ -folds as

$$N(\phi_{\text{F}}) = \frac{1}{\beta_{\text{F}}} \ln (|Ai(\phi_{\text{F}})|) + N_0. \quad (4.32)$$

---

<sup>3</sup>Here we only analyse the model around  $a_1$ ,  $a'_1 \approx -1.02$ , and  $a'_2 \approx -3.25$  points.

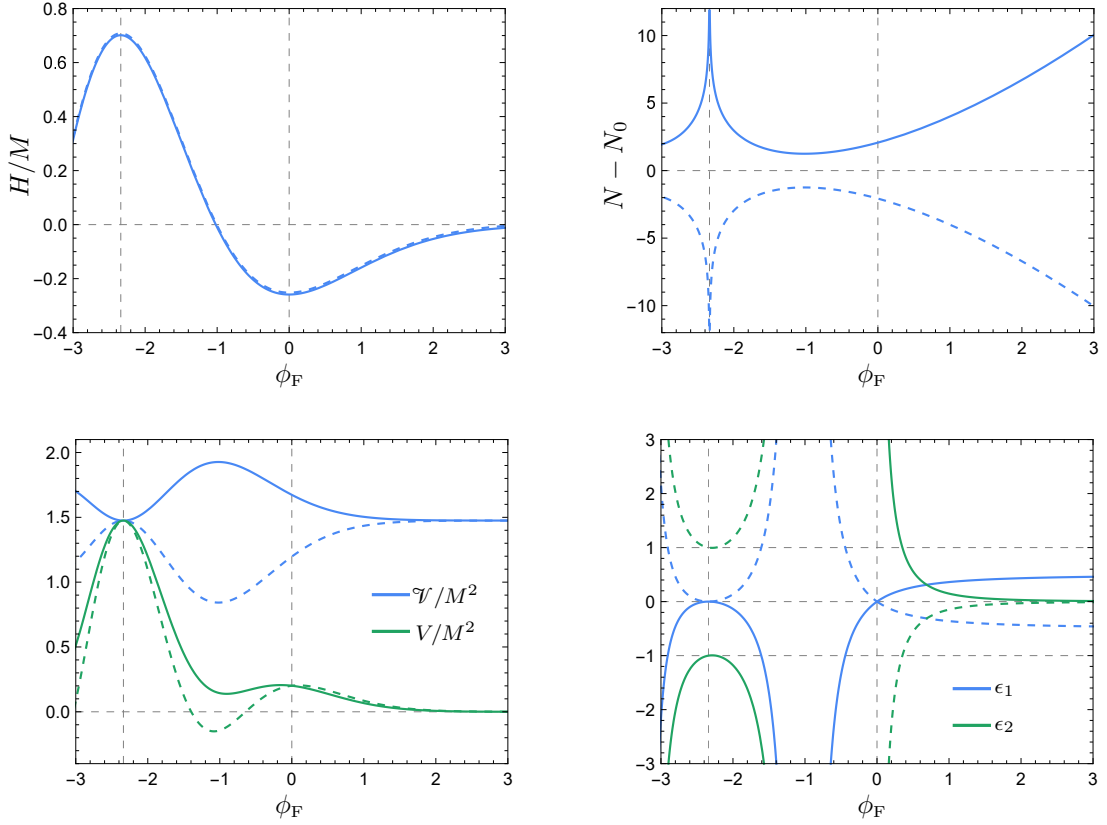


**Figure 4.** The plots of the Hubble parameter (4.31) (top left panel), number of  $e$ -folds (4.32) (top right panel), potential (4.33) and effective potential (4.35) (bottom left panel), and slow-roll parameters (4.36) and (4.37) (bottom right panel), once for  $\beta_F = -0.5$  and  $\gamma = 1$  (solid lines) and once for  $\beta_F = 0.5$  and  $\gamma = -1$  (dashed lines). The parameter  $\mathcal{V}_0$  in effective potential is taken to be 1.475. Two vertical grid lines in all panels correspond to two  $H_{,\phi}$  zeros at  $\phi_F = 0$  and  $\phi_F = a_1 \approx -2.34$ .

The plot of  $N(\phi_F)$  can be seen in the top right panel of Figure 4. We see that  $N(\phi_F)$  is singular at  $\phi_F = a_1$ , where  $H_{,\phi} \rightarrow 0$ , whereas at  $\phi_F = 0$  it is continuous and finite. It is because  $\mathcal{F} = \gamma\phi$  also tends to zero at  $\phi_F = 0$ , making  $H_{,\phi}/\mathcal{F}$  non-zero (see equation (4.13)). As a result, we expect quasi-canonical behavior at  $\phi_F = a_1$  but not at  $\phi_F = 0$ .

To derive the potential we can use equations (4.10) to get

$$V = M^2 [\beta_F \phi_F Ai(\phi_F)^2 + 3Ai'(\phi_F)^2]. \quad (4.33)$$

Equations (4.9) and (4.11) give the gradient of effective potential in the form of

$$\mathcal{V}_{,\phi} = -\frac{M^2 \beta_F (\beta_F + 3)}{\bar{\beta}_F} Ai(\phi_F) Ai'(\phi_F). \quad (4.34)$$

Fortunately, we can also integrate this relation to find the effective potential as

$$\mathcal{V} = \frac{M^2 \bar{\beta}_F (\beta_F + 3)}{\gamma} Ai(\phi_F)^2 + \mathcal{V}_0, \quad (4.35)$$

where  $\mathcal{V}_0$  is the constant of integration. Potential (4.33) and effective potential (4.35) are

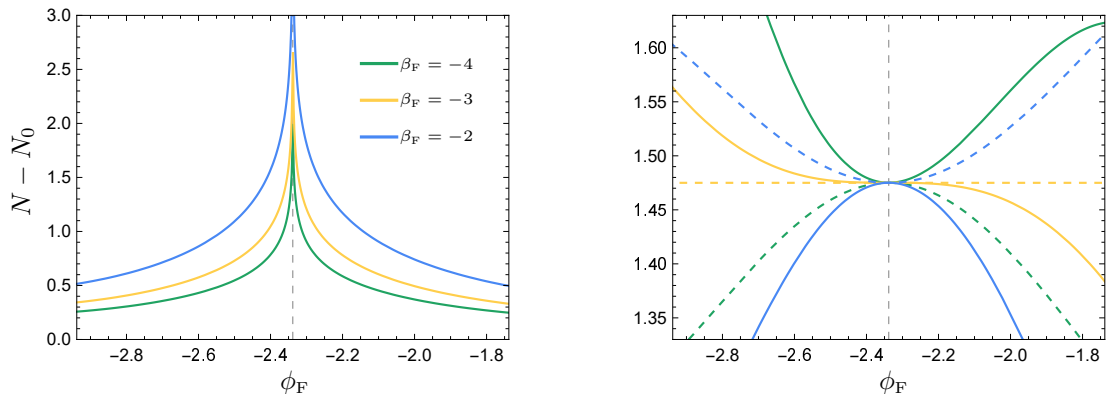


**Figure 5.** Another plot of the number of  $e$ -folds (4.32) (left panel), potential (4.33) (solid lines in right panel), and effective potential (4.35) (dashed lines in right panel) for  $\gamma = 1$  and  $\mathcal{V}_0 = 1.475$ . Vertical grid line at  $\phi_F = a_1$  corresponds to singularities of  $N(\phi_F)$  functions.

plotted in Figure 4 (bottom left panel). The effective potential shows a roller-coaster profile with plateau-like regions connected to steep cliffs. Effective potential extrema are located at  $a_s$  and  $a'_s$  which correspond to zeros of  $H_{,\phi}$  and  $H$ , respectively. We recall that in FCR models the effective potential is not directly proportional to  $\mathcal{F}$  and its concavity at extrema depends only on the sign of the parameter  $\beta_F$ . This is not the case for the potential. In Figure 4 we see that for  $\beta_F = -0.5$  the effective potential is convex around  $\phi_F = a_1$  but for  $\beta_F = 0.5$  it is concave. However, potential is concave in both cases.

Depending on the field initial value, one can think of different inflationary scenarios. In the case of  $\beta_F = -0.5$ , the singularity of  $N(\phi)$  plot at  $a_1$  (and similarly at  $a_s$ ) shows that if the analytic field (that is described by constant  $\beta_F$ ) starts at the neighbourhood of  $\phi_F = a_1$ , it will eventually rest at  $a_1$ . For  $\phi_F > a'_1$ , however, the field moves toward the positive infinity. The field in  $\beta_F = 0.5$  case always rolls in the opposite direction to the  $\beta_F = -0.5$  case. It is important to note that  $\mathcal{F} = 0$ , which in our example happens at  $\phi_F = 0$ , is the singular point of the FCR condition (4.27), which means our solutions are not viable around this point and the field cannot surpass it.

Next we derive and analyze slow-roll parameters. Using definition (2.4) and equations (4.9) and (4.31), for the first and second slow-roll parameters we find

$$\epsilon_1 = -\beta_F \phi_F \left( \frac{Ai(\phi_F)}{Ai'(\phi_F)} \right)^2, \quad (4.36)$$

$$\epsilon_2 = \beta_F \left[ 2 + \frac{1}{\phi_F} \left( \frac{Ai(\phi_F)}{Ai'(\phi_F)} \right) - 2\phi_F \left( \frac{Ai(\phi_F)}{Ai'(\phi_F)} \right)^2 \right]. \quad (4.37)$$

Figure 4 (bottom right panel) illustrates these parameters. At  $\phi_F = a_1$ ,  $\epsilon_1$  is approaching zero, while  $\epsilon_2$  is roughly  $2\beta_F$ . When  $\beta_F = -0.5$ , the field moves toward the extrema at  $a_1$ , where we observe quasi-canonical behavior, whereas when  $\beta_F = 0.5$ , the field moves away from  $a_1$  point, which means we gradually leave the quasi-canonical phase. When  $\beta_F$  is positive,  $\epsilon_1$  grows in time and we can find points where the first slow-roll parameter reaches 1 and inflation ends. Additionally, since we have  $\epsilon_2 \approx 2\beta_F$  when  $\phi_F \rightarrow a_1$ , choosing  $\beta_F < -1$  can potentially lead to a burst in the power spectrum and the formation of primordial black holes. We will talk more about this mechanism in another example in section 5.3.

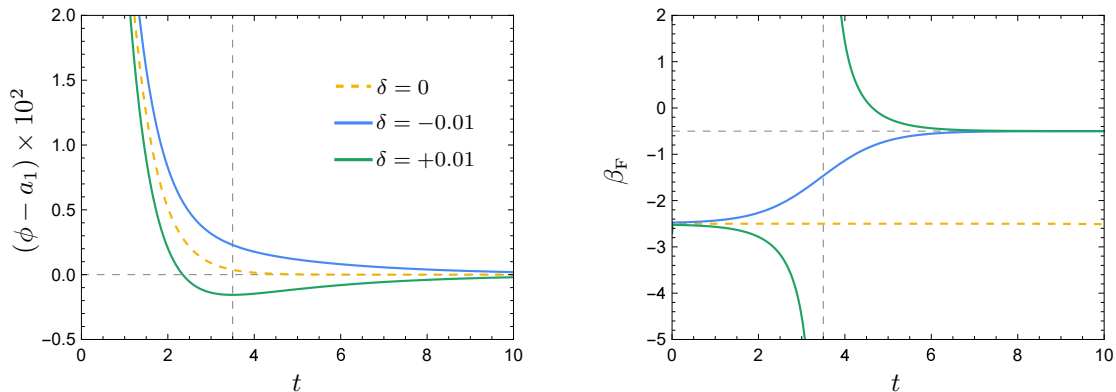


**Figure 6.** We have numerically integrated the field equation (4.4) for  $\beta_{\text{F}} = -2.5$ ,  $\gamma = 1$ , and  $M = 1$ , to evaluate the time evolution of the field (left panel) and the constant-roll parameter  $\beta_{\text{F}} = \ddot{\phi}/(H\dot{\phi})$  (right panel), in order to assess the stability of the constant-roll and propagation solution (4.31) under small perturbations. Initial values for the field and its velocity are taken as  $-2$  and  $-0.295 - \delta$ , respectively. Vertical grid lines correspond to the extremum of  $\dot{\phi}$  in the  $\delta = +0.01$  case. The horizontal grid line in the right panel shows the corresponding dual attractor solution  $\beta_{\text{F}} = -0.5$ .

In Figure 4 we showed how the concavity of potential and effective potential changes around  $\beta_{\text{F}} = 0$ . In Figure 5 (right panel) we plotted the potential and effective potential again, this time for  $\beta_{\text{F}} = -2, -3$ , and  $-4$ , around the critical point  $\phi_{\text{F}} = a_1$ , to show how the concavity changes around  $\beta_{\text{F}} = -3$ . We can see that the potential is convex for  $\beta_{\text{F}} = -4$  and concave for  $\beta_{\text{F}} = -2$ . In each case, since  $\mathcal{F}$  is negative, the concavity of effective potential is in the opposite direction of the potential. When  $\beta_{\text{F}} = -3$ , we have  $\mathcal{V}_{,\phi\phi} = \mathcal{V}_{,\phi} = 0$  and effective potential is flat throughout. There is, however, only one point (at the singularity of  $N(\phi_{\text{F}})$ ) where the first and second derivatives of potential are zero. Actually, we do not have a flat USR like potential for any choice of the constant-roll parameter  $\beta_{\text{F}}$ . To study the USR limit of this model, one should use PCR condition or equivalently HCR condition.

To assess the stability of the model, we employ the methodology outlined in reference [15], imposing a small perturbation that deviates the field evolution from the analytic solution corresponding to a constant  $\beta_{\text{F}}$ . If the model is stable, it should be capable of returning to the constant-roll scenario after a small deviation. The evolution of the field and the constant-roll parameter  $\beta_{\text{F}}$  under small perturbations in the field velocity are plotted in Figure 6. We observe that in the unperturbed constant-roll case, the field ultimately settles at the extrema of the effective potential, with the constant-roll parameter  $\beta_{\text{F}} = -2.5$  remaining unchanged throughout. However, when the absolute value of the initial field velocity  $|\dot{\phi}_0|$  is slightly reduced, the model promptly transitions to the corresponding dual attractor solution  $\beta_{\text{F}} = -0.5$  (see (4.15)) and then settles at the extrema. The situation is a little different when we slightly increase  $|\dot{\phi}_0|$ . In this case, as the field reaches the extrema of the effective potential, where  $\beta_{\text{F}}$  approaches  $-3c_s^2$ , it possesses sufficient kinetic energy to surpass this point. After surpassing the extrema, the field velocity gradually diminishes until it completely stops and reverses its direction. The model then immediately falls into the attractor dual solution  $\beta_{\text{F}} = -0.5$  and eventually comes to rest at the extrema.

We now discuss the HCR solution (4.30). We consider a special case with  $C_4 = 0$  as

$$H(\phi_{\text{H}}) = M \cosh\left(\phi_{\text{H}}^{3/2}\right), \quad (4.38)$$

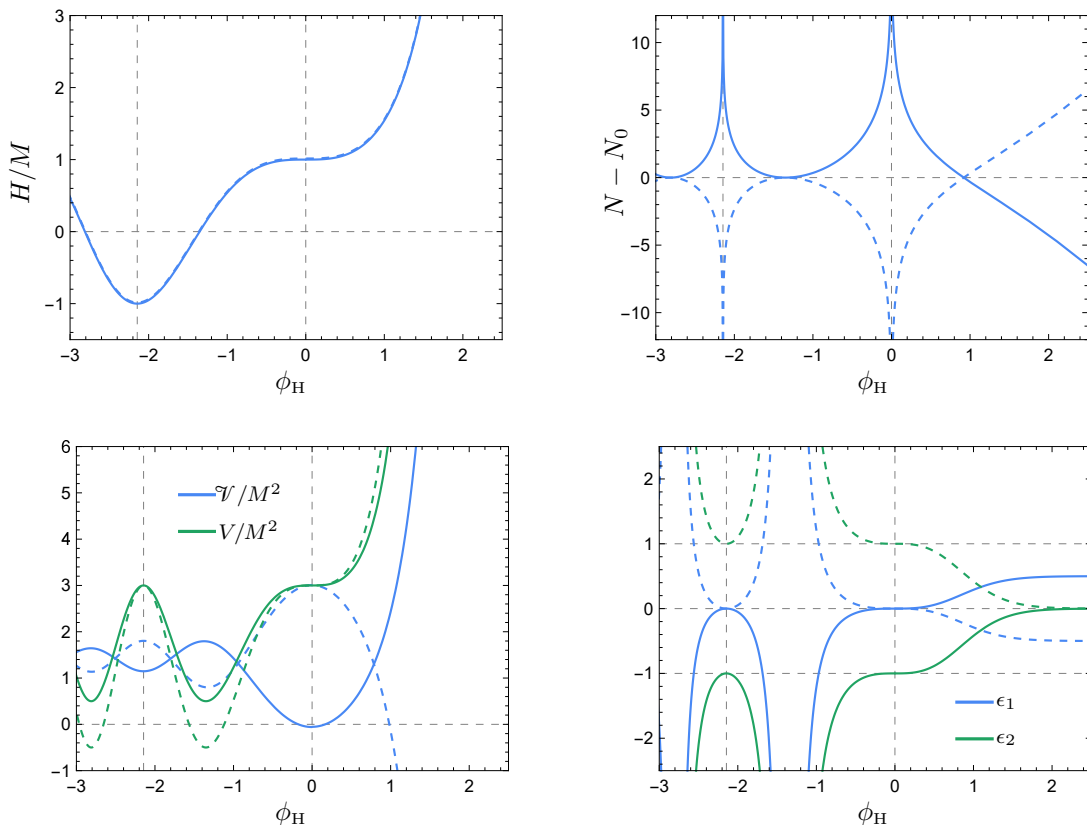


**Figure 7.** The plots of the Hubble parameter (4.38) (top left panel), number of  $e$ -folds (4.39) (top right panel), potential (4.40) and effective potential (4.42) (bottom left panel), and slow-roll parameters (4.44) and (4.45) (bottom right panel), once for  $\beta_F = -0.5$  and  $\gamma = 1$  (solid lines) and once for  $\beta_F = 0.5$  and  $\gamma = -1$  (dashed lines). The parameter  $\mathcal{V}_0$  in effective potential is taken to be 1.475. Two vertical grid lines in all panels correspond to two  $H_{,\phi}$  zeros at  $\phi_F = d_0 = 0$  and  $\phi_F = d_2 \approx -2.15$ .

where for convenience we have define  $M \equiv C_3$ ,  $\bar{\beta}_H \equiv \sqrt[3]{-2\gamma\beta_H/9}$ , and  $\phi_H \equiv \bar{\beta}_H\phi$ . For negative and positive  $\beta_H$  the Hubble parameter (4.38) corresponds to the (2.13) and (2.14) cases, respectively. We have plotted this parameter for  $\beta_F = -0.5$  with  $\gamma = 1$ , as well as  $\beta_F = 0.5$  with  $\gamma = -1$  in Figure 7 (top left panel). Likewise to the FCR case, these two scenarios share a common Hubble parameter but have different dynamical trends. In these specific choices, the parameter  $\bar{\beta}_H$  is real and positive. This implies that for negative values of  $\phi_H$ , the Hubble parameter (4.38) adopts a sinusoidal form, while for positive  $\phi_H$  values, it takes on a hyperbolic form. To pinpoint the critical points of the model, we introduce a new parameter  $d_n$ , defined as  $d_n = -(n\pi/2)^{2/3}$ . With this definition, zeros of Hubble parameter (4.38) are located at  $\phi_H = d_{2s+1}$  and zeros of its derivative,  $H_{,\phi} \propto \sqrt{\phi_H} \sinh(\phi_H^{3/2})$ , are located at  $\phi_H = d_{2s}$ , where  $s$  is a non-negative integer. This section focuses on the model's dynamics around  $\phi_H = d_0 = 0$  and the first extrema points of the Hubble parameter and its derivative on the negative  $\phi_H$  axis at  $\phi_H = d_2 \approx -2.15$  and  $d_1 \approx -1.35$ , respectively.

Using relation (4.25), for the number of  $e$ -folds we find

$$N(\phi_H) = \frac{1}{\beta_F} \ln \left( \left| \sinh \left( \phi_H^{3/2} \right) \right| \right) + N_0. \quad (4.39)$$

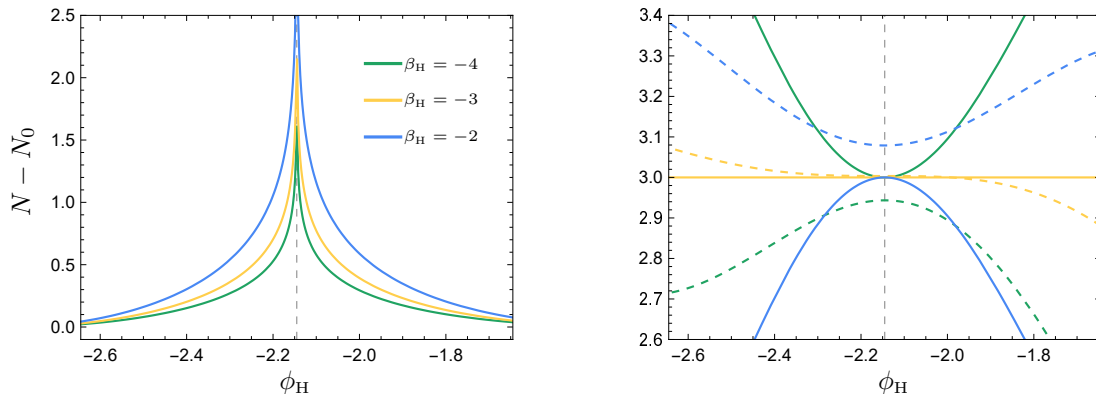


**Figure 8.** Another plot of the number of  $e$ -folds (4.39) (left panel), potential (4.40) (solid lines in right panel), and effective potential (4.42) (dashed lines in right panel) for  $\gamma = 1$  and  $\mathcal{V}_0 = 3.6$ . Vertical grid line at  $\phi_F = d_2 \approx -2.15$  corresponds to singularities of  $N(\phi_H)$  functions.

The plot of this parameter is presented in Figure 7 (top right panel). In contrast to the FCR case, we find that while parameter  $\mathcal{F}$  approaches zero at  $\phi_F = 0$ , the number of  $e$ -folds exhibits a singularity at this point. This is because while the first term in equation (4.25) remains finite at this limit, the second term,  $\ln \mathcal{F}$ , diverges.

Using (4.17) for the potential we get

$$V = \frac{1}{2} M^2 \left[ (\beta_H + 3) \cosh \left( 2\phi_H^{3/2} \right) - \beta_H + 3 \right]. \quad (4.40)$$

For the derivative of effective potential we use the equation (4.23) to obtain

$$\mathcal{V}_{,\phi} = \frac{M^2 \bar{\beta}_H^2}{2\gamma \phi_H^2} \left[ 3(\beta_H + 3) \phi_H^{3/2} \sinh \left( 2\phi_H^{3/2} \right) - 2\beta_H \sinh^2 \left( \phi_H^{3/2} \right) \right]. \quad (4.41)$$

Integrating this equation, the effective potential is driven as

$$\mathcal{V} = \frac{M^2 \bar{\beta}_H}{2\gamma \phi_H} \left[ 3\phi_H^{3/2} \left( E_{\frac{2}{3}} \left( 2\phi_H^{3/2} \right) - E_{\frac{2}{3}} \left( -2\phi_H^{3/2} \right) \right) + 2\beta_H \sinh^2 \left( \phi_H^{3/2} \right) \right] + \mathcal{V}_0, \quad (4.42)$$

where  $\mathcal{V}_0$  is the constant of integration and  $E_n(z)$  is the exponential integral which is defined by

$$E_n(z) = \int_1^\infty \frac{e^{-zt}}{t^n} dt. \quad (4.43)$$

Potential (4.40) and effective potential (4.42) are plotted in the bottom left panel of Figure 7. Extrema of effective potential are located at  $d_s$ , corresponding to zeros of the Hubble parameter and its derivative (see equation (4.23)). Comparing the effective potentials in Figures 4 and 7 around the extrema of the Hubble parameter ( $a_1$  point in the FCR case and the  $d_2$  point in the HCR case), we observe that the concavity of the effective potential in the HCR case resembles that of the FCR case. This is because, as we mentioned, at this critical point the derivatives of the effective potential in the FCR and PCR conditions are approximately equal, and the concavity of the effective potential is solely determined by the constant-roll parameter, regardless of the parameter  $\mathcal{F}$ . The concavity of the potential at  $d_2$  point, however, depends on the sign of  $\mathcal{F}$ , which is why in both cases potential is concave. In

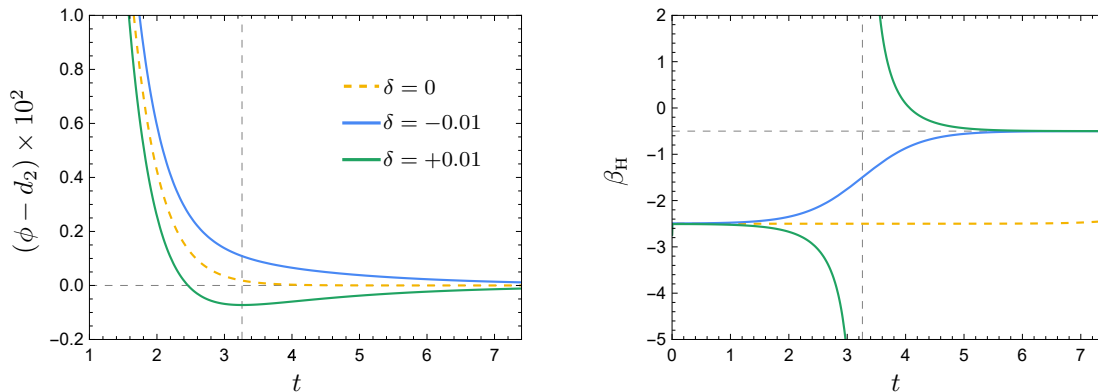


**Figure 9.** We have numerically integrated the field equation (4.4) for  $\beta_{\text{H}} = -2.5$ ,  $\gamma = 1$ , and  $M = -1$ , to evaluate the time evolution of the field (left panel) and the constant-roll parameter  $\beta_{\text{H}} = \ddot{H}/(H\dot{H})$  (right panel), in order to assess the stability of the constant-roll and propagation solution (4.38) under small perturbations. Initial values for the field and its velocity are taken as  $-2$  and  $-1.36 - \delta$ , respectively. Vertical grid lines correspond to the extremum of  $\dot{\phi}$  in the  $\delta = +0.01$  case. The horizontal grid line in the right panel shows the corresponding dual attractor solution  $\beta_{\text{H}} = -0.5$ .

the vicinity of  $\phi_{\text{H}} = 0$ , where the sign of parameter  $\mathcal{F}$  changes, the concavity of the potential undergoes a transition, but the concavity of the effective potential remains unchanged, again emphasizing that the effective potential is unaffected by the  $\mathcal{F}$  function.

To derive the slow-roll parameters as a function of field, we can use equations (4.16). We will have:

$$\epsilon_1(\phi_{\text{H}}) = \beta_{\text{H}} \tan^2\left(\phi_{\text{H}}^{3/2}\right), \quad (4.44)$$

$$\epsilon_2(\phi_{\text{H}}) = 2\beta_{\text{H}} \sec^2\left(\phi_{\text{H}}^{3/2}\right). \quad (4.45)$$

The bottom right panel of Figure 7 represents these parameters. As we can see, at critical points  $\phi_{\text{H}} = d_{2s}$ , the model exhibits the quasi-canonical behavior with  $\epsilon_1$  approaching zero and  $\epsilon_2 \approx 2\beta_{\text{H}}$ . When  $\beta_{\text{H}}$  is negative, field moves toward extrema at  $d_{2s}$ , while for positive  $\beta_{\text{H}}$  it moves away from these points. Therefore, similar to the FCR case, depending on the initial value of the field we will have different inflationary scenarios. In  $\beta_{\text{H}} < 0$  case, the field generally moves toward the extrema of the Hubble parameter (corresponding to singularities of the  $N(\phi_{\text{H}})$ ) at  $d_{2s}$  points, where we observe the quasi-canonical behavior, while in  $\beta_{\text{H}} > 0$  case, the field moves away from these points, gradually leaving the quasi-canonical phase and exits the inflation when  $\epsilon_1$  reaches one. The exception is when both  $\beta_{\text{H}}$  and initial value of the field are positive. In this case, field moves toward the positive infinity.

To analyze the concavity of the potential and effective potential near  $\beta_{\text{H}} = -3$ , we have also plotted these parameters for  $\beta_{\text{H}} = -4, -3$ , and  $-2$ , in the vicinity of the critical point  $\phi_{\text{H}} = d_2$  in Figure 8. A comparison of Figures 5 and 8 reveals that despite the general dissimilarity of potential and effective potential in the HCR case from the FCR, their concavity mirrors that of the FCR case. We also see that, unlike the FCR case, where the potential never maintained a USR profile, here we have a flat potential for  $\beta_{\text{H}} = -3$ , highlighting the effectiveness of the PCR condition for exploring the USR limit of a model.

To check the stability of the model, we have numerically evaluated and plotted the dynamics of the field and the constant-roll parameter  $\beta_{\text{H}}$  in response to slight perturbations in

the field velocity in Figure 9. Similarly to the FCR case, we find that in the unperturbed case the constant-roll parameter  $\beta_{\text{H}}$  retains a constant value  $-2.5$  throughout the evolution, and upon imposing a tiny perturbation to the initial conditions, the model swiftly transitions into the corresponding dual attractor solution with  $\beta_{\text{H}} = -2.5$ , and the field eventually settles at the extremum of the effective potential at  $\beta_{\text{H}} = -0.5$ . Despite their shared features, it is essential to acknowledge that the FCR and HCR cases are not equivalent, as the transition trajectory is influenced by both the constant-roll condition and the parameter  $\mathcal{F}$ . For instance, as mentioned earlier, the value of the field velocity when the field passes the extrema of effective potential in the FCR case is independent of the form of the function  $\mathcal{F}$ , whereas it is dependent on  $\mathcal{F}$  in the HCR case (see equations (4.11) and (4.23)).

## 5 Constant-Roll Kinetically Driven Inflation

In this section we discuss the  $k$  inflation scenario [68–73] as an example of models with varying sound speed that lead to three distinct solutions for the constant-roll conditions discussed in section 3. The equations of motion for the FCR and HCR conditions will be solved analytically to find two sets of constant-roll solutions. However, we lack the analyticity for the PCR condition, so we can only treat it numerically. For a better comparison between our three constant-roll conditions, we will introduce and analyze a concrete inflationary scenario consisting of multiple constant-roll stages where the power spectrum increases significantly and primordial black holes (PBHs) are formed. For each constant-roll condition, the power spectrum and other relevant parameters will be derived numerically and compared.

In the  $k$  inflation we have

$$P(X, \phi) = X + \frac{\gamma}{2}X^2 - V(\phi) = \frac{\dot{\phi}^2}{2} \left( 1 + \frac{1}{4}\gamma\dot{\phi}^2 \right) - V(\phi). \quad (5.1)$$

Using this relation in equations (3.2), (3.3), and (3.4), for Friedmann equation and equations of motion we find

$$3H^2 = \frac{\dot{\phi}^2}{2} \left( 1 + \frac{3}{4}\gamma\dot{\phi}^2 \right) + V, \quad (5.2)$$

$$\dot{H} = -\frac{\dot{\phi}^2}{2} \left( 1 + \frac{1}{2}\gamma\dot{\phi}^2 \right), \quad (5.3)$$

$$\ddot{\phi} \left( 1 + \frac{3}{2}\gamma\dot{\phi}^2 \right) + 3H\dot{\phi} \left( 1 + \frac{1}{2}\gamma\dot{\phi}^2 \right) + V_{,\phi} = 0. \quad (5.4)$$

Action of  $k$  inflation (5.1) is clearly different from the constant propagation model (4.1). Thus, the model is expected to have a variable sound speed. Equation (3.5) can be used to determine sound speed as

$$c_s^2 = \frac{1 + \gamma X}{1 + 3\gamma X}. \quad (5.5)$$

At this point, we constrain the model using constant-roll conditions (3.7), (3.9), and (3.13).

Using relation  $Q = P + V = X + \frac{\gamma}{2}X^2$  we can write

$$\text{FCR: } \frac{\ddot{\phi}}{H\dot{\phi}} = \beta_{\text{F}}, \quad (5.6)$$

$$\text{HCR: } \frac{\ddot{H}}{2H\dot{H}} = \beta_{\text{H}} \Rightarrow \frac{\ddot{\phi} \left(1 + \gamma\dot{\phi}^2\right)}{H\dot{\phi} \left(1 + \frac{1}{2}\gamma\dot{\phi}^2\right)} = \beta_{\text{H}}, \quad (5.7)$$

$$\text{PCR: } \frac{\ddot{\phi}}{H\dot{\phi}} = c_s^2\beta_{\text{V}} - \frac{c_s^2 \left(\dot{\phi}^2 Q_{,X\phi} - Q_{\phi}\right)}{H\dot{\phi} Q_{,X}} \Rightarrow \frac{\ddot{\phi} \left(1 + \frac{3}{2}\gamma\dot{\phi}^2\right)}{H\dot{\phi} \left(1 + \frac{1}{2}\gamma\dot{\phi}^2\right)} = \beta_{\text{V}}, \quad (5.8)$$

where we have used equation (5.3) to eliminate  $\dot{H}$  and  $\ddot{H}$  from equations. Since three constant-roll conditions are different, we expect to find three different sets of solutions. However, when these conditions approach  $\gamma\dot{\phi}^2 \gg 1$  and  $\gamma\dot{\phi}^2 \ll 1$  limits, they become similar, which we will discuss in detail in the next subsection.

### 5.1 Quasi-Canonical Phase

In the limit of  $\gamma\dot{\phi}^2 \ll 1$  the constant  $k$  inflation (5.1) reduces to the canonical case  $P(X, \phi) \approx X - V(\phi)$ , while in the limit of  $\gamma\dot{\phi}^2 \gg 1$  it takes the following form:

$$P(X, \phi) \approx \frac{\gamma}{2}X^2 - V(\phi). \quad (5.9)$$

In the canonical limit  $\gamma\dot{\phi}^2 \ll 1$ , three constant-roll conditions (5.6), (5.7), and (5.8) become identical and we have  $\beta_{\text{F}} = \beta_{\text{H}} = \beta_{\text{V}}$ . On the other hand, in  $\gamma\dot{\phi}^2 \gg 1$  limit, when relation (5.9) holds, our constant-roll conditions become

$$\frac{\ddot{\phi}}{H\dot{\phi}} = \beta_{\text{F}}, \quad 2\frac{\ddot{\phi}}{H\dot{\phi}} = \beta_{\text{H}}, \quad 3\frac{\ddot{\phi}}{H\dot{\phi}} = \beta_{\text{V}}. \quad (5.10)$$

The three constant-roll conditions can be seen to be similar again when  $6\beta_{\text{F}} = 3\beta_{\text{H}} = 2\beta_{\text{V}}$ . This behavior was already expected. Comparing (5.9) with (4.1), we realize that in  $\gamma\dot{\phi}^2 \gg 1$  limit,  $k$  inflation reduces to a constant propagation model with  $c_s = 1/\sqrt{3}$  and  $\mathcal{F} = \gamma/2$ , and we anticipate encountering the same quasi-canonical behavior observed in that context. As we discussed in section 4, in a constant propagation model with constant  $\mathcal{F}$  three constant-roll conditions are analogous (see equation (4.7) and the discussion in the next paragraph). It is also noteworthy that according to the definition of the PCR condition, USR occurs at  $\beta_{\text{V}} = -3$ , which in (5.9) case corresponds to  $\beta_{\text{H}} = -2$  and  $\beta_{\text{F}} = -1$  (compare it with the canonical case that USR happens at  $\beta_{\text{F}} = \beta_{\text{H}} = \beta_{\text{V}} = -3$ ).

We recall for in the case of FCR condition  $\dot{\phi}$  grows rapidly for  $\beta_{\text{F}} > 0$ , while it decays rapidly for  $\beta_{\text{F}} < 0$ . In  $k$  inflation,  $\gamma\dot{\phi}^2$  can become much larger than 1 at the early stages of inflation by choosing a large  $\gamma$ . At this stage, the approximation (5.9) will be viable. If  $\beta_{\text{F}}$  is negative, as  $\dot{\phi}$  decays and  $\gamma$  is constant, the first term in (5.1) will eventually surpass the second term, leading to the canonical case  $P(X, \phi) \approx X - V(\phi)$ . In other words, our model naturally transits into the canonical case. Obviously, if  $\gamma$  is too large or  $\beta_{\text{F}}$  is too small (which results in a slow decaying speed), there may not be enough time for the model to transit into the canonical case during inflation. The situation is opposite when  $\beta_{\text{F}}$  is positive and  $\dot{\phi}$  is growing. In this case, since  $X$  is growing rapidly, the second term in equation (5.1)

will finally become dominant. That means we can start the inflation with canonical case and then move on to (5.9) case.

In the limit of  $\gamma\dot{\phi}^2 \gg 1$ , equations (5.2) and (5.3) are simplified as

$$3H^2 = \frac{3}{8}\gamma H^4 \phi_{,N}^4 + V, \quad (5.11)$$

$$H_{,N} = -\frac{1}{4}\gamma H^3 \phi_{,N}^4, \quad (5.12)$$

where we have written all derivatives in terms of  $N$ . Since this model is a special case of constant propagation model (4.1), all results derived in section 4 apply here as well. That means we can use Hubble parameters (2.13), (2.14), (2.15), and (2.29), potentials (4.18),(4.19),(4.20), and (4.21), slow-roll parameters (2.19), (2.23), (2.27), and (2.34), and spectral indexes (2.35), (2.36), and (2.37). What we were unable to derive in section 4, was the field and accordingly  $V(\phi)$ . For solutions (2.13), (2.14), (2.15), and (2.29) we can integrate equations (5.11) or (5.12) to find the following solutions for the field respectively:

$$\phi(N) = \pm \left( -\frac{64}{\gamma M^2 \beta_{\text{H}}^3} \right)^{1/4} e^{\frac{1}{2}\beta_{\text{H}}N} {}_2F_1 \left( \frac{1}{4}, \frac{1}{2}; \frac{5}{4}; -e^{2\beta_{\text{H}}N} \right) + \phi_c, \quad (5.13)$$

$$\phi(N) = \pm \left( \frac{64}{\gamma M^2 \beta_{\text{H}}^3} \right)^{1/4} e^{\frac{1}{2}\beta_{\text{H}}N} {}_2F_1 \left( \frac{1}{4}, \frac{1}{2}; \frac{5}{4}; e^{2\beta_{\text{H}}N} \right) + \phi_c, \quad (5.14)$$

$$\phi(N) = \pm \left( -\frac{64}{\gamma M^2 \beta_{\text{H}}^3} \right)^{1/4} e^{\frac{1}{2}\beta_{\text{H}}N} {}_2F_1 \left( \frac{1}{4}, \frac{1}{2}; \frac{5}{4}; e^{2\beta_{\text{H}}N} \right) + \phi_c, \quad (5.15)$$

$$\phi(N) = \pm \left( \frac{32}{\gamma M^2} \right)^{1/4} \sqrt{-N} + \phi_c, \quad (5.16)$$

where  ${}_2F_1$  is the hypergeometric function. To find  $V(\phi)$  we need to solve the above equations to find  $N$  as a function of  $\phi$ . However, due to the presence of the hypergeometric function in solutions (5.13), (5.14), and (5.15),  $N(\phi)$  cannot be derived. For the fourth solution (5.16),  $V(\phi)$  can be found as

$$V(\phi) = \frac{3}{4}M^2 \left( \sqrt{\frac{\gamma M^2}{2}}(\phi - \phi_c)^2 - 1 \right). \quad (5.17)$$

With all the solutions in hand, we can now discuss which ranges of parameters  $\beta_{\text{H}}$  and  $N$  lead to inflation. Here the Hubble and slow-roll parameters are identical to those in the canonical case, so allowed ranges of  $\beta_{\text{H}}$  and  $N$  are also identical unless the field becomes imaginary. In the inflationary range, solutions (5.13), (5.14), and (5.16) are real, but solution (5.15) is imaginary. However, the imaginary part of this solution is constant, so it can always be absorbed by redefining the integration constant as  $\phi_c \rightarrow \phi_c - \Im(\phi(N))$ . Therefore, these fields do not further constrain the parameters' ranges.

Now that we have fields, we can compare  $\gamma\dot{\phi}^2$  with 1 to see how long the approximation (5.9) remains valid. For solutions (5.13) and (5.15) we can write

$$\gamma\dot{\phi}^2 = \gamma H^2 \phi_{,N}^2 = 2M \sqrt{\gamma |\beta_{\text{H}}|} e^{\beta_{\text{H}}(N - N_{\text{ini}})}, \quad (5.18)$$

where we have assumed that inflation starts at  $N = N_{\text{ini}}$ . Note that this relation is consistent with the general relation (3.8) since we have  $\beta_{\text{H}} = 2\beta_{\text{F}}$  in  $\gamma\dot{\phi}^2 \gg 1$  limit. We now define

parameter  $\delta$  such that the approximation (5.9) starts to break at the critical point  $\gamma\dot{\phi}_{\text{cri}}^2 = \delta$ . Using equation (5.18), we can find the number e-fold at the critical point as

$$N_{\text{cri}} = \frac{1}{2\beta_{\text{H}}} \ln \left( \frac{\delta^2}{4\gamma M^2 |\beta_{\text{H}}|} \right) + N_{\text{ini}}. \quad (5.19)$$

As an example, if  $\delta = 10$ ,  $M = 1$ ,  $\gamma = 10^5$ , and  $\beta_{\text{H}} = -0.5$  then  $N_{\text{cri}} \approx 7.6 + N_{\text{ini}}$ . Therefore, approximation (5.9) is valid for the first 7.6 e-folds of the inflation. After this point the first and second terms in relation (5.1) are comparable and we must use exact solutions. When  $\dot{\phi}$  continues to decay, the model will eventually reach the canonical case.

Note that relation (5.18) can also be used for solution (5.14). However, in this solution  $\beta_{\text{H}}$  is positive and  $\dot{\phi}$  is growing rather than decaying. Which means inflation can be started from the canonical case and then transit to (5.9) case. To evaluate the number e-fold at the critical point (the moment when canonical approximation starts to break) we use solution (2.20) to write

$$\gamma\dot{\phi}^2 = \gamma H^2 \phi_{,N}^2 = 2\gamma M^2 \beta_{\text{H}} e^{2\beta_{\text{H}}(N-N_{\text{ini}})}, \quad (5.20)$$

where we have assumed that inflation starts at  $N = N_{\text{ini}}$ . Again, this condition is consistent with relation (3.8) since in the canonical limit we have  $\beta_{\text{H}} = \beta_{\text{F}}$ . Similar to (5.19), by defining a proper  $\delta$  parameter, we can find the number e-fold at the critical point as

$$N_{\text{cri}} = \frac{1}{2\beta_{\text{H}}} \ln \left( \frac{\delta}{2\gamma M^2 \beta_{\text{H}}} \right) + N_{\text{ini}}. \quad (5.21)$$

For instance, for  $\delta = 0.1$ ,  $M = 1$ ,  $\gamma = 10^{-5}$ , and  $\beta_{\text{H}} = 0.5$  we find  $N_{\text{cri}} \approx 9.2 + N_{\text{ini}}$ . That means canonical approximation is valid at the beginning of inflation until it breaks at around 9.2 e-folds. After this point we must use exact solutions. As  $\dot{\phi}$  grows, we gradually enter the next phase where we can use approximate relation (5.9). For the last solution (5.16), since  $\ddot{\phi}$  is zero and  $\dot{\phi}$  constant, there is no transition between (5.9) and canonical case.

## 5.2 Exact Solutions

We will now solve equations of motion analytically without considering any approximations. Writing time derivatives in equations (5.2) and (5.3) in terms of  $N$  we will have

$$3H^2 = \frac{H^2 \phi_{,N}^2}{2} \left( 1 + \frac{3\gamma}{4} H^2 \phi_{,N}^2 \right) + V, \quad (5.22)$$

$$H_{,N} = -\frac{H \phi_{,N}^2}{2} \left( 1 + \frac{\gamma}{2} H^2 \phi_{,N}^2 \right). \quad (5.23)$$

Let us first derive the Hubble parameter for all three constant-roll conditions (5.6), (5.7), and (5.8). As we discussed in section 3, for the HCR condition it is possible to derive Hubble parameter even without knowing the exact form of the action. As a result, we can again use solutions (2.13), (2.14), (2.15), and (2.29) for Hubble parameters. For the PCR condition (5.8) Hubble parameter cannot be found analytically. For the FCR condition, after writing the time derivatives in (5.6) in terms of  $N$  and removing  $\phi_{,N}$  and  $\phi_{,NN}$  using equation (5.23), we get

$$\begin{aligned} & \gamma H_{,N}^4 + H \left( -8\gamma\beta_{\text{F}} H_{,N}^3 + 2\gamma H_{,N}^2 H_{,NN} + 2\beta_{\text{F}} H_{,NN} - 4\beta_{\text{F}}^2 H_{,N} \right) \\ & + \gamma H^2 (H_{,NN} - 4\beta_{\text{F}} H_{,N})^2 + 2\beta_{\text{F}} H_{,N}^2 = 0. \end{aligned} \quad (5.24)$$

Integrating out, we can find the following solution for this equation:

$$H^2 = \frac{1}{2\gamma\beta_{\text{F}}} \left[ \tilde{M}^2 - \left( e^{2\beta_{\text{F}}(N-\tilde{N})} + 1 \right)^2 \right], \quad (5.25)$$

where  $\tilde{M}$  and  $\tilde{N}$  are two complex constants, which similar to our discussion in section 2, they should be chosen properly so that (5.25) leads to a viable inflationary scenario. When  $\beta_{\text{F}}$  is exactly zero, we will find the solution (2.29) again. Thus, we identified eight constant-roll solutions. Four solutions from (5.6), three solutions from (5.7), and one solution for  $\beta_{\text{F}} = \beta_{\text{H}} = 0$  case. In order to compare the FCR and HCR conditions, we can proceed to derive other parameters of the model. But, the PCR condition can only be treated numerically. In the next subsection, we investigate a practical inflationary scenario and derive the power spectrum and other relevant parameters numerically to compare all three constant-roll conditions.

### 5.3 PBH Formation

It is clarified that a sharp enhancement in the amplitude of the power spectrum between small and large scales can be responsible for the production of PBHs [57]. To achieve such an enhancement one needs to look beyond the slow-roll limit and/or canonical case. In constant  $k$  model, by choosing a large value for the constant-roll parameter, the slow-roll approximation can easily be violated. Moreover, the model is non-canonical and has variable sound speed, which affect the power enhancement.

To understand the enhancement mechanism of power spectrum we look at the differential equation governing the curvature perturbation,

$$u_k'' + 2\frac{z'}{z}u_k' + k^2u_k = 0, \quad (5.26)$$

where for  $z'/z$  we have

$$\frac{z'}{z} = aH \left( 1 + \frac{\epsilon_2}{2} + q_1 \right), \quad (5.27)$$

and  $q_1$  is defined in equation (A.4). Equation (5.26) is similar to the equation of motion of a harmonic oscillator with friction. When  $z'/z$  becomes negative, the friction term acts as a driving term, resulting in a sharp increase in the power spectrum. In the canonical constant-roll model, when we have  $\epsilon_2 \approx 2\beta$ , to achieve negative  $z'/z$  we need to choose  $\beta < -1$ . In the non-canonical case with variable sound speed  $q_1$  is non-zero and should be taken into account.

Now we construct a four-stage constant-roll model, capable of enhancing power spectrum, satisfying CMB constraints, and providing a graceful exit from inflation. First, we discuss the scenario for the canonical case, then we apply it to  $k$  inflation under the three constant-roll conditions (5.6), (5.7), and (5.8).

We start by constructing a multiple-stage constant-roll parameter as follows:

$$\beta(N) = -\frac{493}{10} \left( \frac{2000}{1953} + \tanh(3(N-15)) \right) \left( \frac{39}{40} - \tanh(3(N-20.5)) \right) \left( \frac{137}{136} + \tanh(3(N-60)) \right). \quad (5.28)$$

This parameter (plotted in panel (a) of Figure 10) describes four stages of constant-roll inflation (with  $\beta = -0.017, -1.45, 0.018,$  and  $5$ , respectively). The stages are connected using proper smooth functions. The constant-roll parameter is set to  $-0.017$  in the first

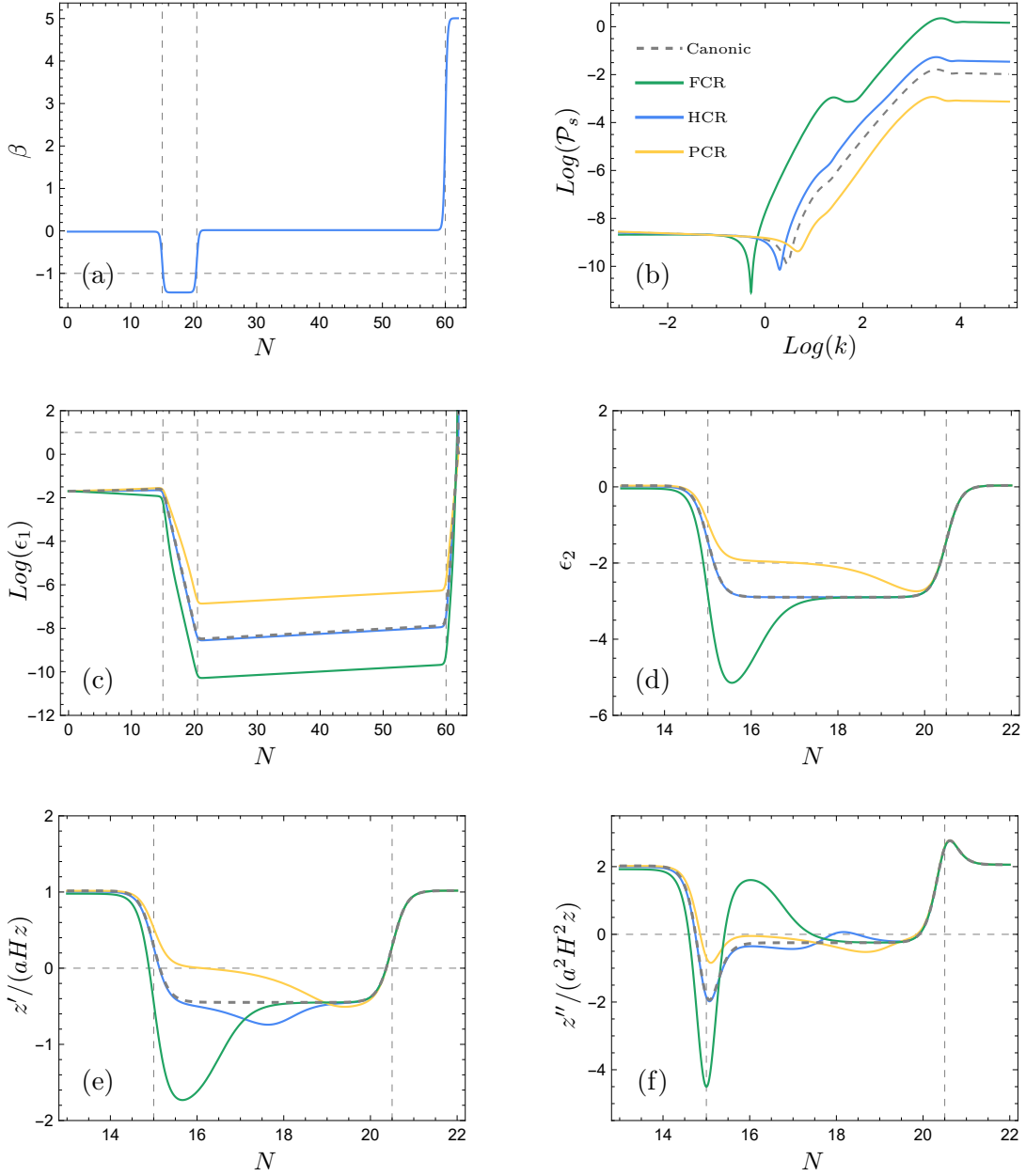


**Figure 10.** (a) constant-roll parameter  $\beta$ , (b) power spectrum  $\mathcal{P}_s$ , (c) first slow-roll parameter  $\epsilon_1$ , (d) second slow-roll parameter  $\epsilon_2$ , (e) parameter  $z'/(aHz)$ , and (f) effective potential  $z''/(a^2 H^2 z)$  for the constant  $k$  inflation. In all panels except panel (a), green, blue, and yellow lines represent FCR, HCR, and PCR conditions, respectively. Dashed gray lines correspond to the canonical case. There are four constant-roll stages with  $\beta(N) \approx -0.017, -1.45, 0.018, \text{ and } 5$  separated by three vertical grid lines at  $N = 10, 20.5, \text{ and } 60$  e-folds. The initial stage of the scenario is a slow-roll case that meets the CMB constraints at the pivot point  $k_{\text{cmb}} = 0.05 \text{Mpc}^{-1}$ . In the second stage the constant-roll parameter is chosen smaller than  $-1$  in order to induce the formation of PBHs, but larger than  $-3/2$  to preserve the attractor behavior. Upon reaching the desired amplitude of power spectrum, we enter another slow-roll stage to prevent overproduction of PBHs. During the final stage of the scenario, the constant-roll parameter is large and positive, resulting in a quick exit from inflation.

stage in order to comply with Planck data (see discussion after equation (2.36)). At this stage we normalized the power spectrum to meet the CMB constraints [74],  $\mathcal{P}_s = 2.1 \times 10^{-9}$  at  $k_{\text{cmb}} = 0.05 \text{Mpc}^{-1}$ . After 15 e-folds we switch to a large  $\beta$  stage responsible for enhancing the power spectrum. We take the constant-roll parameter smaller than  $-1$  to have negative  $z'/z$ , but larger than  $-3/2$  in order to preserve the attractor behavior of the model. At 21.5 e-folds, when the power has increased around  $10^7$  times, we end this stage. The third stage is another slow-roll stage with  $\beta = 0.018$  that is compatible with Planck data (see discussion after equation (2.35)). At the end, we enter a short stage with large positive  $\beta$  at 60 e-folds, that leads to a sharp increase in  $\dot{\phi}$  and accordingly  $\epsilon_1$ , allowing us to reach  $\epsilon_1 = 1$  and exit inflation gracefully.

In the canonical case, we use parameter (5.28) in equation (2.6) and solve the equations of motion and Mukhanov-Sasaki equation (A.2) numerically to derive power spectrum and dynamical parameters. The results are illustrated in Figure 10 (dashed gray lines). As can be seen, the power has increased by about  $10^7$  times, which is appropriate for PBH formation as suggested in references [57, 58]. In this scenario, when  $\beta$  changes, we might automatically switch to another constant-roll solution. Solutions (2.15) and (2.13) can be used to describe the first and second stages respectively, and solution (2.14) can be used to describe the last two stages.

For  $k$  inflation the situation is more complicated. In this model we start inflation in  $\gamma\dot{\phi}^2 \gg 1$  phase when (5.9) is valid. In the first stage, since  $\beta$  is small and  $\dot{\phi}$  decays slowly, there is not enough time to transit to the canonical case. During the second stage,  $|\beta|$  increases significantly leading to a quick decay in  $\dot{\phi}$  and the transition to the canonical case. During the third stage  $\beta$  becomes positive and  $\dot{\phi}$  begins to grow. However, since  $\beta$  is small we remain in the canonical case throughout. In the last stage, as  $\beta$  is large and positive,  $\dot{\phi}$  grows dramatically fast and we transit back to  $\gamma\dot{\phi}^2 \gg 1$  limit before exiting inflation.

After using (5.28) in three constant-roll conditions (5.6), (5.7), and (5.8), we numerically solved dynamical equations to derive the power spectrum and dynamical parameters. Figure 10 shows the results (the green, blue, and yellow lines represent FCR, HCR, and PCR conditions, respectively). It should be noted that here we want to compare three constant-roll conditions within a single scenario. We are concerned about the effect of changing the constant-roll condition on the model, not the compatibility of each power spectrum with the data.

Looking at panels (c) and (d) of Figure 10, it is evident that the slow-roll parameters for the HCR condition are identical to those for the canonical case. It is due to the fact that for the HCR condition slow-roll parameters can be derived irrespective of action. However, since the sound speed is not constant, the power spectrum will be different. As can be seen in panels (e) and (f) of Figure 10, parameters  $z'/(aH z)$  and  $z''/(a^2 H^2 z)$  for the HCR condition differ slightly from the canonical case, which is the direct result of varying sound speed (also see equations (5.27) and (A.3)).

Panel (c) of Figure 10 also shows that in all stages of the scenario except the third stage, the slope of  $\text{Log}(\epsilon_1)$  differs for three constant-roll conditions. This is because at third stage we reach the canonical case regardless of our choice of constant-roll condition. This point becomes more clear when we look at the second slow-roll parameter in panel (d) of Figure 10. Despite reaching a single path at about 20 e-folds,  $\epsilon_2$  functions are different in earlier times when we have not reached the canonical limit yet. In early times of inflation when approximation (5.9) is valid, in order to get similar results from three constant-roll conditions we must choose  $6\beta_{\text{F}} = 3\beta_{\text{H}} = 2\beta_{\text{V}}$  (see equation (5.10)), but our choice is  $\beta_{\text{F}} =$

$\beta_{\text{H}} = \beta_{\text{V}} = \beta(N)$ , where  $\beta(N)$  is defined in (5.28). However, when we enter the canonical phase, our choice  $\beta_{\text{F}} = \beta_{\text{H}} = \beta_{\text{V}} = \beta(N)$  leads to similar results for three constant-roll conditions (see discussion after equation (5.9)). Therefore, we can expect a similar dynamic for three constant-roll conditions at third stage since we are in the canonical limit.

Looking at panel (e) of Figure 10, we see that in all cases  $z'/(aHz)$  transiently changes sign, which is necessary to enhance the power spectrum. The more it goes toward negative signs the stronger will be the driving force that enhances the power. Therefore, by looking at  $z'/(aHz)$  we expect that the FCR condition, followed by the HCR and PCR conditions, will result in greater power spectrum enhancement. Which is the case as can be seen in panel (b) of Figure 10.

## 6 Summary and Conclusion

This study explored three methods for imposing the constant-roll condition on non-canonical models. We used a general action as a toy model to introduce three distinct constant-roll conditions, which are all equivalent in the canonical limit but may lead to different results in non-canonical cases. In the first approach, in which a more conventional form of the constant-roll condition in the literature is used, the condition was defined to ensure that the inflaton rolling rate remains constant throughout the inflation. Imposing another type of the constant-roll condition ensures a constant  $\epsilon_2$  in the model. This second condition enabled us to derive the time profile of the Hubble and slow-roll parameters analytically, even without knowing the exact form of the action. For models with constant sound speed the power spectrum and spectral index of the model were also derived. In these two approaches, we may not obtain a flat USR potential for any value of the constant-roll parameter. Therefore, in our third approach, we defined the constant-roll condition so that we recover the USR model when constant-roll parameter approaches  $-3$ . Obviously, this condition is useful in studying the USR limit of a model. We dubbed these three conditions the FCR, HCR, and PCR conditions, respectively. These conditions were examined to determine under which conditions on action these purportedly distinct conditions result in homologous models and when they differ.

To provide a clear example, we investigated a class of non-canonical models characterized by the constant sound speed, denoted as "constant propagation inflation", within the framework of our generalized constant-roll formalism. We demonstrated that within this class of models, the HCR and PCR conditions display homologous behavior. In a particular case with  $c_s = 1$  (corresponding to a class of models known as k/G inflation), we identified two distinct sets of constant-roll solutions under the HCR and FCR conditions. While these solutions generally differ, we showed that in specific limits where  $H_{,\phi}$  approaches zero and the field settles at the extrema of the effective potential, both FCR and HCR models exhibit similar quasi-canonical behavior, where slow-roll parameters mimic their canonical counterparts, though the action generally deviates from the canonical form. We also conducted a full dynamical analysis of the constant-roll parameter under small perturbations in the field velocity to assess the stability of our exemplar of constant propagation model. We determined that for a range of the constant-roll parameters the analytic solutions are unstable and will generally transition to their corresponding dual attractor constant-roll solutions. We noted that the transition trajectory is universal in FCR case but is contingent upon the form of the action in HCR scenario.

We also investigated another non-canonical action within the framework of the constant-roll scenario. We observed that when constant-roll parameter is negative, the model transitions automatically from a quasi-canonical phase to a canonical constant-roll phase, and when constant-roll parameter is positive it evolves in the opposite direction. We noted that while the nature of these two phases remains independent of the chosen constant-roll condition, the transition trajectory is highly dependent on this choice. We subsequently introduced a multi-stage "constant  $k$ " scenario and conducted a numerical assessment of the system parameters and the power spectrum. This exploration demonstrated how modifying the constant-roll condition can significantly impact the model's outcomes, emphasizing on the sensitivity of the system to the chosen constant-roll condition.

We stress that the constant-roll conditions we defined in this work are not unique. Mathematically, one can define an infinite number of constant-roll conditions for a non-canonical model, each leading to the conventional constant-roll condition  $\ddot{\phi} = \beta H \dot{\phi}$  in the canonical limit. We believe this is an intriguing flexibility of the model that has not yet been adequately examined. The study of a non-canonical model under the conventional constant-roll condition can indeed provide some insights. However, other forms of the constant-roll condition may also provide valuable information that should not be overlooked.

## Acknowledgements

We acknowledge the financial support of the research council of the University of Tehran.

## A The Turning Point of $n_s$ and $f_{NL}^{re}$

In this appendix we go into the mathematical details of the power spectrum and the contribution of field redefinition to non-Gaussianity in the constant-roll scenario. We explain why perturbations suddenly change behavior at  $\beta = -3/2$ . We begin by considering the general action (3.1),

$$S = \frac{1}{2} \int d^4x \sqrt{-g} [R + 2P(X, \phi)]. \quad (\text{A.1})$$

In this model, the Mukhanov-Sasaki variable  $v_k$ , which is related to the mode function of curvature perturbations  $u_k$  through the relation  $v_k \equiv zu_k$ , satisfies the following equation [75, 78, 79]:

$$v_k'' + \left( c_s^2 k^2 - \frac{z''}{z} \right) v_k = 0, \quad (\text{A.2})$$

where  $z \equiv a\sqrt{2\epsilon_1}/c_s$  and  $c_s$  is the sound speed defined in equation (3.5). In general,  $z''/z$  term in the above equation can be written as follows:

$$\frac{z''}{z} = a^2 H^2 \left( 2 - \epsilon_1 + \frac{3}{2}\epsilon_2 + \frac{1}{4}\epsilon_2^2 - \frac{1}{2}\epsilon_1\epsilon_2 + \frac{1}{2}\epsilon_2\epsilon_3 + 3q_1 - \epsilon_1q_1 + \epsilon_2q_1 + q_1^2 + q_1q_2 \right), \quad (\text{A.3})$$

where parameters  $q_j$  are defined as

$$q_1 = \frac{d \ln c_s}{dN}, \quad q_{j+1} = \frac{d \ln q_j}{dN}. \quad (\text{A.4})$$

At super Hubble scales,  $k \ll aH$ , we can neglect the  $c_s^2 k^2$  term in equation (A.2) and integrated it out to find

$$u = C_1 + C_2 \int \frac{d\tau}{a^2 \epsilon_1} = C_1 + \frac{C_2}{a_0^3 H} \int \frac{dN}{e^{3N} \epsilon_1}. \quad (\text{A.5})$$

This approximate form is useful for analyzing the evolution of modes in large scales.

We now constrain the model under the HCR condition (3.9),

$$\frac{\ddot{H}}{2H\dot{H}} = \beta_{\text{H}}. \quad (\text{A.6})$$

By integrating this equation we find the slow-roll parameters plotted in Figure 1. However, since we are interested in the behavior of perturbations around  $\beta_{\text{H}} = -3/2$  point, we will only consider solution (2.13). To solve equation (A.2), it is also necessary to derive  $q_j$  parameters (A.4), which cannot be obtained without knowing the form of the action. For simplicity we consider the constant propagation model (4.1), where the sound speed is constant. Therefore,  $q_j$  parameters are zero, and slow-roll parameters are approximated as  $\epsilon_1 \approx 0$ ,  $\epsilon_2 \approx 2\beta_{\text{H}}$ , and  $\epsilon_3 \approx 0$  in large positive  $N$ . Using these results equation (A.2) simplifies to

$$v_k'' + \left( c_s^2 k^2 - \frac{\nu^2 - 1/4}{\tau^2} \right) v_k = 0, \quad (\text{A.7})$$

where we have defined parameter  $\nu$  as

$$\nu \equiv \sqrt{(\beta_{\text{H}} + 1)(\beta_{\text{H}} + 2) + \frac{1}{4}} = \left| \beta_{\text{H}} + \frac{3}{2} \right|. \quad (\text{A.8})$$

Solving equation (A.7), we find the standard mode function as follows:

$$v_k(\tau) = \frac{\sqrt{-\pi\tau}}{2} H_{\nu}^{(1)}(-c_s k \tau). \quad (\text{A.9})$$

This mode is normalized such that at early times we recover the Bunch-Davis vacuum

$$\lim_{k\tau \rightarrow -\infty} v_k = \frac{1}{\sqrt{2k}} e^{-ik\tau}. \quad (\text{A.10})$$

We can now evaluate the dimensionless power spectrum of curvature perturbations. With solution (A.9), we will have

$$\mathcal{P}_s(k) \equiv \frac{k^3}{2\pi^2} |u_k|^2 = \frac{H^2}{8\pi^2 \epsilon_1} \left( \frac{k}{aH} \right)^3 \frac{\pi}{2} \left| H_{\nu}^{(1)}(-c_s k \tau) \right|^2. \quad (\text{A.11})$$

In  $\tau \rightarrow 0$  limit we use the asymptotic formula  $\lim_{x \rightarrow 0} H_{\nu}^{(1)}(x) \simeq -\frac{i}{\pi} \Gamma(\nu) (x/2)^{-\nu}$  to get

$$\mathcal{P}_s(k) \approx \frac{H^2}{8\pi^2 \epsilon_1} \frac{2^{2\nu-1} [\Gamma(\nu)]^2}{\pi} \left( \frac{c_s k}{aH} \right)^{3-2\nu}. \quad (\text{A.12})$$

Accordingly, the spectral index is  $n_s - 1 = 3 - 2\nu = 3 - 2|\beta_{\text{H}} + 3/2|$ , which is consistent with equation (2.35).

Our next step will be the evaluation of the contribution of field redefinition to non-Gaussianity around  $\beta_{\text{H}} = -3/2$  in order to investigate its sudden behavior change. In the calculations of non-Gaussianity it is shown that a field redefinition as  $\zeta \rightarrow \zeta_n + f(\zeta_n)$  can significantly simplify the interaction Hamiltonian. In general, for a  $P(X)$  model (A.1),  $f(\zeta)$  is given by

$$\begin{aligned} f(\zeta) &= \frac{\epsilon_2}{4c_s^2} \zeta^2 + \frac{1}{c_s^2 H} \zeta \dot{\zeta} + \frac{1}{4a^2 H^2} [ -(\partial\zeta)(\partial\zeta) + \partial^{-2}(\partial_i \partial_j (\partial_i \zeta \partial_j \zeta)) ] \\ &+ \frac{1}{2a^2 H} [ (\partial\zeta)(\partial\chi) - \partial^{-2}(\partial_i \partial_j (\partial_i \zeta \partial_j \chi)) ]. \end{aligned} \quad (\text{A.13})$$

If  $\beta_H > -3/2$ , modes will freeze out on super Hubble scales. Therefore, all derivative terms in above equation will vanish and will not contribute to non-Gaussianity. If  $\beta_H < -3/2$ , however,  $\dot{\zeta}$  term is non-vanishing and will contribute. Therefore, for the calculation of the correlation function we only consider the first two terms in equation (A.13). After field redefinition  $\zeta \rightarrow \zeta_n + \frac{\epsilon_2}{4c_s^2}\zeta_n^2 + \frac{1}{c_s^2 H}\zeta_n\dot{\zeta}_n$  the three point function becomes

$$\begin{aligned} \langle \zeta(\mathbf{x}_1) \zeta(\mathbf{x}_2) \zeta(\mathbf{x}_3) \rangle &= \langle \zeta_n(\mathbf{x}_1) \zeta_n(\mathbf{x}_2) \zeta_n(\mathbf{x}_3) \rangle \\ &+ \frac{\epsilon_2}{2c_s^2} (\langle \zeta_n(\mathbf{x}_1) \zeta_n(\mathbf{x}_2) \rangle \langle \zeta_n(\mathbf{x}_1) \zeta_n(\mathbf{x}_3) \rangle + \text{sym}) \\ &+ \frac{1}{c_s^2 H} (\langle \dot{\zeta}_n(\mathbf{x}_1) \zeta_n(\mathbf{x}_2) \rangle \langle \zeta_n(\mathbf{x}_1) \zeta_n(\mathbf{x}_3) \rangle + \text{sym}) + \mathcal{O}(\langle \zeta_n^5(\mathbf{x}) \rangle), \end{aligned} \quad (\text{A.14})$$

where  $\mathcal{O}(\langle \zeta_n^5(\mathbf{x}) \rangle)$  indicates the higher order terms. Writing the above expression in Fourier space and using relation  $\langle \zeta_n(k_1) \zeta_n(k_2) \rangle = (2\pi)^3 \delta(k_1 + k_2) u_{k_1} u_{k_2}^*$ , for the contribution of field redefinition to three point function we find

$$\begin{aligned} (2\pi)^3 \delta^{(3)}(\mathbf{x}_1 + \mathbf{x}_2 + \mathbf{x}_3) &\left[ \frac{\epsilon_2}{2c_s^2} (|u(\mathbf{x}_2)|^2 |u(\mathbf{x}_3)|^2 + \text{sym}) + \right. \\ &\left. \frac{1}{c_s^2 H} (|u(\mathbf{x}_2)|^2 \dot{u}(\mathbf{x}_3) u^*(\mathbf{x}_3) + |u(\mathbf{x}_3)|^2 \dot{u}(\mathbf{x}_2) u^*(\mathbf{x}_2) + \text{sym}) \right]. \end{aligned} \quad (\text{A.15})$$

We now try to find a relationship between  $\dot{u}$  and  $u$ . For this, we use relation  $v = zu$  to write

$$\dot{u} = -uH \left( \frac{\tau v'}{v} + \frac{\epsilon_2}{2} + 1 \right). \quad (\text{A.16})$$

Using solution (A.9) for  $\tau v'/v$  term in the above equation we can write

$$\lim_{\tau \rightarrow 0} \frac{\tau v'}{v} = \lim_{\tau \rightarrow 0} \frac{c_s k \tau H_{\nu+1}^{(1)}(-c_s k \tau)}{H_\nu^{(1)}(-c_s k \tau)} + \nu + \frac{1}{2} \approx -\nu + \frac{1}{2}, \quad (\text{A.17})$$

where again we have used asymptotic relation  $\lim_{x \rightarrow 0} H_\nu^{(1)}(x) \simeq -\frac{i}{\pi} \Gamma(\nu) (x/2)^{-\nu}$  for Hankel function. In the light of equations (A.15), (A.16), and (A.17) the bispectrum and non-Gaussianity parameters can be found as

$$B_s^{re}(k_1, k_2, k_3) = \frac{1}{c_s^2} \left( 2\nu - 3 - \frac{\epsilon_2}{2} \right) \left[ |u_{k_2}(\tau_f)|^2 |u_{k_3}(\tau_f)|^2 + \text{sym} \right], \quad (\text{A.18})$$

$$f_{NL}^{re} = \frac{5}{6c_s^2} \left( 2\nu - 3 - \frac{\epsilon_2}{2} \right) = \frac{5}{6c_s^2} \left( 2 \left| \beta_H + \frac{3}{2} \right| - 3 - \frac{\epsilon_2}{2} \right), \quad (\text{A.19})$$

which for  $c_s = 1$  and  $\epsilon_2 \approx 2\beta_H$  leads to relation (2.38).

## References

- [1] A.D. Linde, *A New Inflationary Universe Scenario: A Possible Solution of the Horizon, Flatness, Homogeneity, Isotropy and Primordial Monopole Problems*, *Phys. Lett. B* **108** (1982) 389.
- [2] K. Sato, *First-order phase transition of a vacuum and the expansion of the Universe*, *Monthly Notices of the Royal Astronomical Society* **195** (1981) 467.

- [3] A.H. Guth, *Inflationary universe: A possible solution to the horizon and flatness problems*, *Phys. Rev. D* **23** (1981) 347.
- [4] A. Albrecht, P.J. Steinhardt, M.S. Turner and F. Wilczek, *Reheating an inflationary universe*, *Phys. Rev. Lett.* **48** (1982) 1437.
- [5] A. Linde, *A new inflationary universe scenario: A possible solution of the horizon, flatness, homogeneity, isotropy and primordial monopole problems*, *Physics Letters B* **108** (1982) 389.
- [6] D.H. Lyth and A. Riotto, *Particle physics models of inflation and the cosmological density perturbation*, *Physics Reports* **314** (1999) 1.
- [7] J. Martin, *What have the Planck data taught us about inflation?*, *Classical and Quantum Gravity* **33** (2016) 034001.
- [8] N. Tsamis and R.P. Woodard, *Improved estimates of cosmological perturbations*, *Physical Review D* **69** (2004) 084005 [[arXiv:astro-ph/0307463](#)].
- [9] W.H. Kinney, *Horizon crossing and inflation with large  $\eta$* , *Physical Review D* **72** (2005) 023515 [[arXiv:gr-qc/0503017](#)].
- [10] M.H. Namjoo, H. Firouzjahi and M. Sasaki, *Violation of non-gaussianity consistency relation in a single-field inflationary model*, *Europhysics Letters* **101** (2013) 39001 [[arXiv:1210.3692](#)].
- [11] J. Martin, H. Motohashi and T. Suyama, *Ultra slow-roll inflation and the non-gaussianity consistency relation*, *Physical Review D* **87** (2013) 023514 [[arXiv:1211.0083](#)].
- [12] H. Motohashi, A.A. Starobinsky and J. Yokoyama, *Inflation with a constant rate of roll*, *Journal of Cosmology and Astroparticle Physics* (2015) 018 [[arXiv:1411.5021](#)].
- [13] L. Anguelova, P. Suranyi and L.R. Wijewardhana, *Systematics of constant roll inflation*, *Journal of Cosmology and Astroparticle Physics* (2018) [[arXiv:1710.06989](#)].
- [14] M.J. Morse and W.H. Kinney, *Large- $\eta$  constant-roll inflation is never an attractor*, *Physical Review D* **97** (2018) [[arXiv:1804.01927](#)].
- [15] W.-C. Lin, M.J. Morse and W.H. Kinney, *Dynamical analysis of attractor behavior in constant roll inflation*, *Journal of Cosmology and Astroparticle Physics* (2019) [[arXiv:1904.06289](#)].
- [16] A. Mohammadi, N. Ahmadi and M. Shokri, *On the constant roll complex scalar field inflationary models*, *Journal of Cosmology and Astroparticle Physics* (2023) 058 [[arXiv:2212.13403](#)].
- [17] H. Motohashi and Y. Tada, *Squeezed bispectrum and one-loop corrections in transient constant-roll inflation*, *arXiv preprint* (2023) [[arXiv:2303.16035](#)].
- [18] N.K. Stein and W.H. Kinney, *Simple single-field inflation models with arbitrarily small tensor/scalar ratio*, *Journal of Cosmology and Astroparticle Physics* (2023) 027 [[arXiv:2210.05757](#)].
- [19] J. Sadeghi and S.N. Gashti, *Anisotropic constant-roll inflation with noncommutative model and swampland conjectures*, *The European Physical Journal C* **81** (2021) 1 [[arXiv:2104.00117](#)].
- [20] H. Firouzjahi, A. Nassiri-Rad and M. Noorbala, *Stochastic ultra slow roll inflation*, *Journal of Cosmology and Astroparticle Physics* (2019) 040 [[arXiv:2009.04680](#)].
- [21] C. Pattison, V. Vennin, H. Assadullahi and D. Wands, *The attractive behaviour of ultra-slow-roll inflation*, *Journal of Cosmology and Astroparticle Physics* (2018) 048 [[arXiv:1806.09553](#)].
- [22] J.T.G. Ghersi, A. Zucca and A.V. Frolov, *Observational constraints on constant roll inflation*, *Journal of Cosmology and Astroparticle Physics* (2019) 030 [[arXiv:1808.01325](#)].
- [23] F. Cicciarella, J. Mabillard and M. Pieroni, *New perspectives on constant-roll inflation*, *Journal of Cosmology and Astroparticle Physics* (2018) 024 [[arXiv:1709.03527](#)].

- [24] Z. Yi and Y. Gong, *On the constant-roll inflation*, *Journal of Cosmology and Astroparticle Physics* (2018) 052 [[arXiv:1712.07478](#)].
- [25] B. Boisseau and H. Giacomini, *Inflationary models that generalize the constant roll constraint*, *Journal of Cosmology and Astroparticle Physics* (2019) 054 [[arXiv:1809.09169](#)].
- [26] V. Oikonomou, *Generalizing the constant-roll condition in scalar inflation*, *International Journal of Geometric Methods in Modern Physics* **19** (2022) 2250099 [[arXiv:2106.10778](#)].
- [27] H. Motohashi and A.A. Starobinsky,  *$f(R)$  constant-roll inflation*, *The European Physical Journal C* **77** (2017) 1 [[arXiv:1704.08188](#)].
- [28] K.E. Bourakadi, Z. Sakhi and M. Bennai, *Observational constraints on tachyon inflation and reheating in  $f(Q)$  gravity*, *arXiv preprint* (2023) [[arXiv:2302.11229](#)].
- [29] Y.-P. Wu, E. Pinetti, K. Petraki and J. Silk, *Baryogenesis from ultra-slow-roll inflation*, *Journal of High Energy Physics* (2022) 1 [[arXiv:2109.00118](#)].
- [30] M. AlHallak, N. Chamoun and M. Eldaher, *Natural inflation with non minimal coupling to gravity in  $R^2$  gravity under the palatini formalism*, *Journal of Cosmology and Astroparticle Physics* (2022) 001 [[arXiv:2202.01002](#)].
- [31] J.C. Garnica, L.G. Gomez, A.A. Navarro and Y. Rodriguez, *Constant-roll inflation in the generalized  $SU(2)$  Proca theory*, *Annalen der Physik* **534** (2022) 2100453 [[arXiv:2109.10154](#)].
- [32] M. Shokri, J. Sadeghi and M.R. Setare, *The generalized  $sl(2, R)$  and  $su(1, 1)$  in non-minimal constant-roll inflation*, *Annals of Physics* **429** (2021) 168487 [[arXiv:2104.01917](#)].
- [33] A. Mohammadi, K. Saaidi and T. Golanbari, *Tachyon constant-roll inflation*, *Physical Review D* **97** (2018) 083006 [[arXiv:1801.03487](#)].
- [34] Q. Gao, Y. Gong and Q. Fei, *Constant-roll tachyon inflation and observational constraints*, *Journal of Cosmology and Astroparticle Physics* (2018) 005 [[arXiv:1801.09208](#)].
- [35] A. Mohammadi, T. Golanbari and K. Saaidi, *Beta-function formalism for  $k$ -essence constant-roll inflation*, *Physics of the Dark Universe* **28** (2020) 100505 [[arXiv:1912.07006](#)].
- [36] V. Oikonomou and F. Fronimos, *Reviving non-minimal horndeski-like theories after  $GW170817$ : kinetic coupling corrected einstein–gauss–bonnet inflation*, *Classical and Quantum Gravity* **38** (2020) 035013 [[arXiv:2006.05512](#)].
- [37] A. Mohammadi, K. Saaidi and H. Sheikahmadi, *Constant-roll approach to noncanonical inflation*, *Physical Review D* **100** (2019) 083520 [[arXiv:1803.01715](#)].
- [38] S.D. Odintsov and V.K. Oikonomou, *Constant-roll  $k$ -inflation dynamics*, *Classical and Quantum Gravity* **37** (2019) 025003 [[arXiv:1912.00475](#)].
- [39] A. Mohammadi, T. Golanbari, S. Nasri and K. Saaidi, *Constant-roll brane inflation*, *Physical Review D* **101** (2020) 123537 [[arXiv:2004.12137](#)].
- [40] M. Shokri, J. Sadeghi and S.N. Gashti, *Quintessential constant-roll inflation*, *Physics of the Dark Universe* **35** (2022) 100923 [[arXiv:2107.04756](#)].
- [41] M. Shokri, M.R. Setare, S. Capozziello and J. Sadeghi, *Constant-roll  $f(R)$  inflation compared with cosmic microwave background anisotropies and swampland criteria*, *The European Physical Journal Plus* **137** (2022) 1 [[arXiv:2108.00175](#)].
- [42] Z. Yi, Y. Gong, M. Sabir et al., *Inflation with Gauss-Bonnet coupling*, *Physical Review D* **98** (2018) 083521 [[arXiv:1804.09116](#)].
- [43] S.V. Chervon, I.V. Fomin and A. Beesham, *The method of generating functions in exact scalar field inflationary cosmology*, *The European Physical Journal C* **78** (2018) 1 [[arXiv:1704.08712](#)].

- [44] E. Elizalde, S. Odintsov, V. Oikonomou and T. Paul, *Logarithmic-corrected  $R^2$  gravity inflation in the presence of kalb-ramond fields*, *Journal of Cosmology and Astroparticle Physics* (2019) 017 [[arXiv:1810.07711](#)].
- [45] A. Awad, W. El Hanafy, G. Nashed, S. Odintsov and V. Oikonomou, *Constant-roll inflation in  $f(T)$  teleparallel gravity*, *Journal of Cosmology and Astroparticle Physics* (2018) 026 [[arXiv:1710.00682](#)].
- [46] A. Karam, L. Marzola, T. Pappas, A. Racioppi and K. Tamvakis, *Constant-roll (quasi-) linear inflation*, *Journal of Cosmology and Astroparticle Physics* (2018) 011 [[arXiv:1711.09861](#)].
- [47] S. Odintsov, V. Oikonomou and L. Sebastiani, *Unification of constant-roll inflation and dark energy with logarithmic  $R^2$ -corrected and exponential  $F(R)$  gravity*, *Nuclear Physics B* **923** (2017) 608 [[arXiv:1708.08346](#)].
- [48] V. Oikonomou, *Reheating in constant-roll  $F(R)$  gravity*, *Modern Physics Letters A* **32** (2017) 1750172 [[arXiv:1706.00507](#)].
- [49] S. Nojiri, S. Odintsov and V. Oikonomou, *Constant-roll inflation in  $F(R)$  gravity*, *Classical and Quantum Gravity* **34** (2017) 245012 [[arXiv:1704.05945](#)].
- [50] S. Panda, A. Rana and R. Thakur, *Constant-roll inflation in modified  $f(R, \phi)$  gravity model using palatini formalism*, *The European Physical Journal C* **83** (2023) 297 [[arXiv:2212.00472](#)].
- [51] I. Antoniadis, A. Lykkas and K. Tamvakis, *Constant-roll in the Palatini- $R^2$  models*, *Journal of cosmology and astroparticle physics* (2020) 033 [[arXiv:2002.12681](#)].
- [52] M. Shokri, J. Sadeghi, M.R. Setare and S. Capozziello, *Nonminimal coupling inflation with constant slow roll*, *International Journal of Modern Physics D* **30** (2021) 2150070 [[arXiv:2104.00596](#)].
- [53] K. El Bourakadi, M. Koussour, G. Otalora, M. Bennai and T. Ouali, *Constant-roll and primordial black holes in  $f(Q, T)$  gravity*, *Physics of the Dark Universe* **41** (2023) 101246 [[arXiv:2301.03696](#)].
- [54] H. Motohashi and A.A. Starobinsky, *Constant-roll inflation in scalar-tensor gravity*, *Journal of Cosmology and Astroparticle Physics* (2019) 025 [[arXiv:1909.10883](#)].
- [55] R. Herrera, M. Shokri and J. Sadeghi, *Galilean constant-roll inflation*, *Physics of the Dark Universe* **41** (2023) 101232 [[arXiv:2206.01264](#)].
- [56] M. Shokri, J. Sadeghi and M.R. Setare, *Constant-roll inflation from a fermionic field*, *Europhysics Letters* **139** (2022) 19001 [[arXiv:2107.03283](#)].
- [57] O. Özsoy and G. Tasinato, *Inflation and primordial black holes*, *Universe* **9** (2023) 203 [[arXiv:2301.03600](#)].
- [58] H. Motohashi, S. Mukohyama and M. Oliosi, *Constant roll and primordial black holes*, *Journal of Cosmology and Astroparticle Physics* (2020) 002 [[arXiv:1910.13235](#)].
- [59] O. Özsoy and G. Tasinato, *On the slope of the curvature power spectrum in non-attractor inflation*, *Journal of Cosmology and Astroparticle Physics* (2020) 048 [[arXiv:1912.01061](#)].
- [60] E. Tomberg, *Stochastic constant-roll inflation and primordial black holes*, *arXiv preprint* (2023) [[arXiv:2304.10903](#)].
- [61] J. Kristiano and J. Yokoyama, *Ruling out primordial black hole formation from single-field inflation*, *arXiv preprint* (2022) [[arXiv:2211.03395](#)].
- [62] S.S. Mishra, E.J. Copeland and A.M. Green, *Primordial black holes and stochastic inflation beyond slow roll:  $I$ -noise matrix elements*, *arXiv preprint* (2023) [[arXiv:2303.17375](#)].
- [63] M.W. Davies, P. Carrilho and D.J. Mulryne, *Non-gaussianity in inflationary scenarios for primordial black holes*, *Journal of Cosmology and Astroparticle Physics* (2022) 019 [[arXiv:2110.08189](#)].

- [64] Y.-P. Wu, E. Pinetti and J. Silk, *Cosmic coincidences of primordial-black-hole dark matter*, *Physical Review Letters* **128** (2022) 031102 [[arXiv:2109.09875](#)].
- [65] A. Karam, N. Koivunen, E. Tomberg, V. Vaskonen and H. Veermäe, *Anatomy of single-field inflationary models for primordial black holes*. *arxiv 2022, arXiv preprint* [[arXiv:2205.13540](#)].
- [66] K.-W. Ng and Y.-P. Wu, *Constant-rate inflation: primordial black holes from conformal weight transitions*, *Journal of High Energy Physics* (2021) 1 [[arXiv:2102.05620](#)].
- [67] J. Lin, Q. Gao, Y. Gong, Y. Lu, C. Zhang, F. Zhang et al., *Primordial black holes and secondary gravitational waves from  $k$  and  $g$  inflation*, *Physical Review D* **101** (2020) 103515 [[arXiv:2001.05909](#)].
- [68] C. Armendariz-Picon, T. Damour and V. Mukhanov,  *$k$ -inflation*, *Physics Letters B* **458** (1999) 209 [[arXiv:hep-th/9904075](#)].
- [69] T. Chiba, T. Okabe and M. Yamaguchi, *Kinetically driven quintessence*, *Physical Review D* **62** (2000) 023511 [[arXiv:astro-ph/9912463](#)].
- [70] C. Armendariz-Picon, V. Mukhanov and P.J. Steinhardt, *Essentials of  $k$ -essence*, *Physical Review D* **63** (2001) 103510 [[arXiv:astro-ph/0006373](#)].
- [71] T. Chiba, *Tracking  $k$ -essence*, *Physical Review D* **66** (2002) 063514 [[arXiv:astro-ph/0206298](#)].
- [72] M. Malquarti, E.J. Copeland, A.R. Liddle and M. Trodden, *A new view of  $k$ -essence*, *Physical Review D* **67** (2003) 123503 [[arXiv:astro-ph/0302279](#)].
- [73] A.D. Rendall, *Dynamics of  $k$ -essence*, *Classical and Quantum Gravity* **23** (2006) 1557 [[arXiv:gr-qc/0511158](#)].
- [74] Y. Akrami, F. Arroja, M. Ashdown, J. Aumont, C. Baccigalupi, M. Ballardini et al., *Planck 2018 results-X. constraints on inflation*, *Astronomy & Astrophysics* **641** (2020) [[arXiv:1807.06211](#)].
- [75] J. Noller and J. Magueijo, *Non-gaussianity in single field models without slow-roll conditions*, *Physical Review D* **83** (2011) [[arXiv:1102.0275](#)].
- [76] J. Maldacena, *Non-gaussian features of primordial fluctuations in single field inflationary models*, *Journal of High Energy Physics* (2003) 013 [[arXiv:astro-ph/0210603](#)].
- [77] V. Olivier et al., *Airy functions and applications to physics*, World Scientific (2010).
- [78] X. Chen, M.-x. Huang, S. Kachru and G. Shiu, *Observational signatures and non-gaussianities of general single-field inflation*, *Journal of Cosmology and Astroparticle Physics* (2007) 002 [[arXiv:hep-th/0605045](#)].
- [79] D. Seery and J.E. Lidsey, *Primordial non-gaussianities in single-field inflation*, *Journal of Cosmology and Astroparticle Physics* (2005) 003 [[arXiv:astro-ph/0503692](#)].